

alone resulted in significant tumor growth suppression compared with mock-treated tumors. The combination of OBP-301 plus radiation produced a more profound and significant inhibition of tumor growth compared with either modality alone in all three types of tumors, despite the difference in treatment schedules (Fig. 4A).

Histopathologic analysis of A549 tumors excised 10 days after the completion of three cycles of either regional radiation or OBP-301 infection revealed the degeneration of tissues and reduced tumor cell density compared with untreated tumors. However, treatment with OBP-301 injection plus radiation yielded massive tissue destruction and further reduction in tumor cell density. Moreover, the cytolytic changes induced by the combination therapy led to the development of hyalinized acellular stroma (Fig. 4B). Terminal deoxyribonucleotidyl transferase-mediated dUTP nick

end labeling (TUNEL) staining showed that combining ionizing radiation with OBP-301 markedly increased the amount of apoptotic cells in A549 tumors excised 3 days after the completion of the treatment (Fig. 4C). OBP-301 plus irradiation apparently increased PARP cleavage in A549 tumors compared with ionizing radiation alone (Fig. 4D).

#### Eradication of established human tumor xenografts by OBP-301 plus radiation

To mimic the clinical characteristics of advanced cancer patients, we established TES xenografts with a 10-fold larger tumor burden. Mice bearing large TES subcutaneous tumors received nine cycles of 2 Gy irradiation followed by intratumoral injection of  $1 \times 10^8$  PFU of OBP-301 three times per week for 3 weeks. Tumors treated with either OBP-301 or ionizing radiation alone exhibited a transient shrinkage,

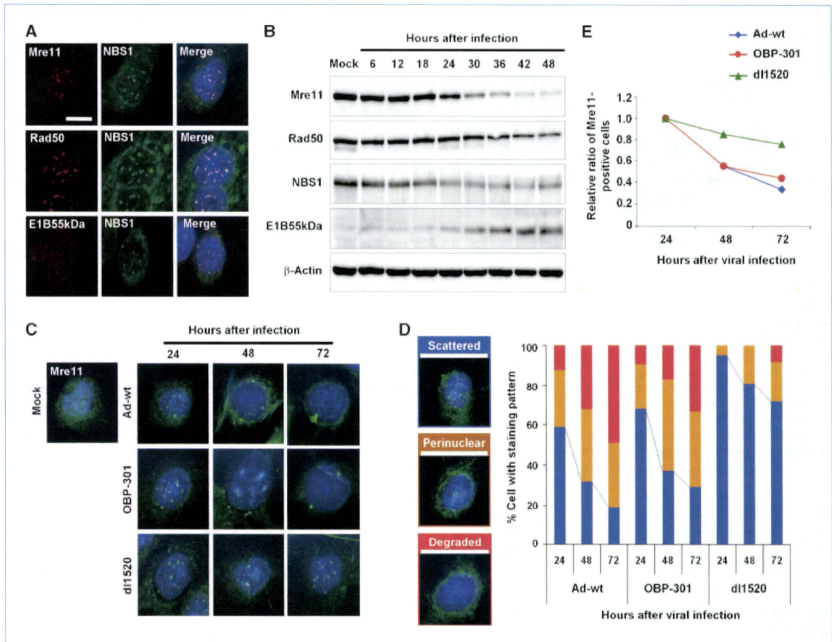


**Figure 2.** Degradation of the MRN complex by E1B55kDa protein. A, A549 cells were infected with OBP-301 at an MOI of 10 and then stained for NBS1 and either Mre11, Rad50, or E1B55kDa 24 h after infection. The localization of these proteins was visualized by confocal laser microscopy. Scale bar, 100  $\mu$ m. B, A549 cells were infected with OBP-301 at an MOI of 10 and collected at the indicated time points after infection. Blots were probed with antibodies for Mre11, Rad50, NBS1, and E1B55kDa. C, A549 cells were infected with either Ad-wt, OBP-301, or dl1520 (Onyx-015) at an MOI of 10; stained for Mre11 at 24, 48, and 72 h after infection; and analyzed by confocal laser microscopy. D, The subcellular distribution of Mre11 protein was classified as scattered, perinuclear, and degraded. The proportions of each pattern were determined 24, 48, and 72 h after viral infection. E, quantification of Mre11-positive cells after OBP-301 infection. The relative ratios of cells with scattered staining are plotted against the amount of time since infection.

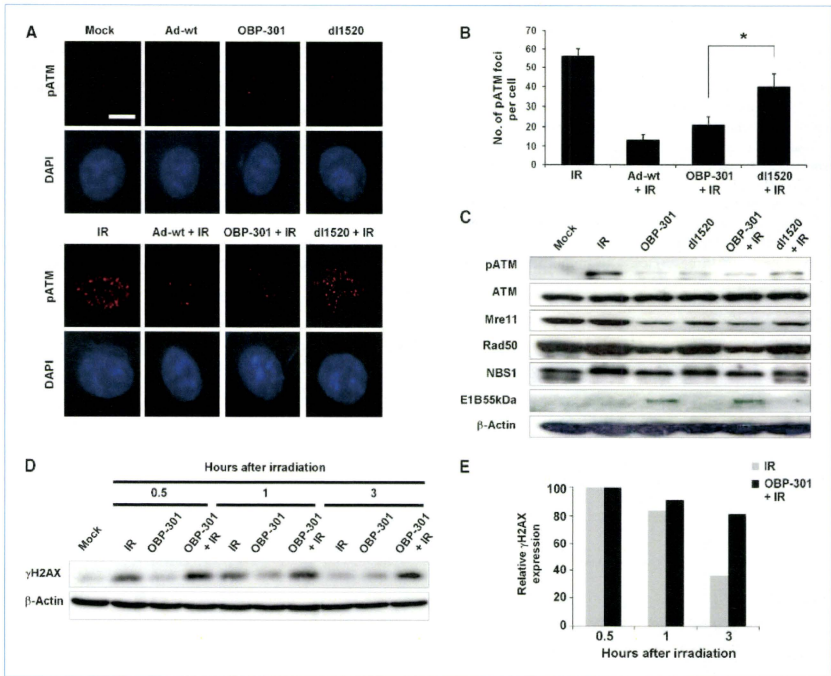


**Figure 3.** Inhibition of DNA repair by E1B55kDa protein through the blockade of radiation-induced ATM autophosphorylation. **A**, A549 cells were infected with either Ad-wt, OBP-301, or d11520 at an MOI of 10 and then irradiated with 10 Gy at 24 h after infection. Nuclear phosphorylated ATM (pATM) foci were visualized 30 min after irradiation by immunofluorescent staining under a confocal laser microscope. Scale bar, 100  $\mu$ m. **B**, quantification of pATM foci in treated A549 cells. The numbers of pATM foci per cell were counted in 10 different cells per group. \*,  $P < 0.01$ . **C**, A549 cells were infected with OBP-301 or d11520 and irradiated with 10 Gy at 24 h after infection. Cells were then subjected to Western blot analysis for pATM, ATM, Mre11, Rad50, NBS1, E1B55kDa, and  $\beta$ -actin 30 min after irradiation. **D**,  $\gamma$ H2AX expression after irradiation in cells with or without OBP-301 infection. A549 cells were infected with OBP-301 at an MOI of 10 and then irradiated with 10 Gy at 24 h after infection. The cells were harvested at 0.5, 1, and 3 h after irradiation and subjected to Western blot analysis for  $\gamma$ H2AX. Note the maintenance of  $\gamma$ H2AX in the presence of OBP-301 infection. **E**, the levels of  $\gamma$ H2AX expression were quantified by densitometric scanning with Image J software. The relative  $\gamma$ H2AX expression is shown as a percentage of the  $\gamma$ H2AX/ $\beta$ -actin value at 30 min after irradiation.

but invariably started to regrow 14 days after the beginning of treatment, whereas OBP-301 plus radiation completely eradicated the established larger TES tumors on day 28 in 9 of 10 mice (Fig. 5A).

Tumors treated with OBP-301 or radiation alone were consistently smaller than tumors of the control cohort of mice (Fig. 5B; Supplementary Fig. S8A). Massive ulceration was noted on the tumor surface after injection of OBP-301, whereas no tumor burden was detected when ionizing radiation was combined with OBP-301 injection. Moreover, histologic analysis revealed the apparent destruction of tumor tissues after OBP-301 injection or ionizing radiation.

However, no residual tumor cells were observed in tumors treated with OBP-301 plus radiation; instead, massive cellular infiltrates were noted (Supplementary Fig. S8B). Mice with tumor eradication significantly recovered their body weight, although there was a gradual decrease in the body weight of the control group (Supplementary Fig. S9).

#### Evaluation of *in vivo* antitumor effects on orthotopic human esophageal cancer model

Finally, we assessed the therapeutic efficacy of intratumoral injection of OBP-301 and local irradiation in an orthotopic human esophageal cancer xenograft model by

using noninvasive whole-body imaging. When TE8 human esophageal cancer cells stably transfected with the luciferase gene (TE8-Luc) were s.c. implanted into nude mice, a correlation was observed between tumor growth (volume) and the luciferase emission level (luminescent intensity; Supplementary Fig. S10). Our preliminary experiments revealed that when TE8-Luc cells were inoculated into the wall of the abdominal esophagus of athymic *nu/nu* mice, esophageal tumors appeared within 3 weeks after tumor injection (Fig. 5C).

Mice bearing macroscopic esophageal tumors were treated with local irradiation at 2 Gy followed by intratumoral injection during laparotomy of  $1 \times 10^8$  PFU of OBP-301 every 2 days for three cycles. The luminescent intensity

of tumors treated with OBP-301 plus radiation was significantly lower than that of mock-treated, irradiated, or OBP-301-injected tumors (Fig. 5D and E). These results suggest that the biochemical interaction of OBP-301 with irradiation can be translated into a potential clinically applicable cancer treatment.

## Discussion

A novel biological property of OBP-301 as a molecular radiosensitizer was verified, referring to a critical role of adenoviral E1B55kDa in inhibiting the DNA damage responses triggered by ionizing radiation. Radiation-induced cell death is dependent on DNA damage and, therefore, inhibition of

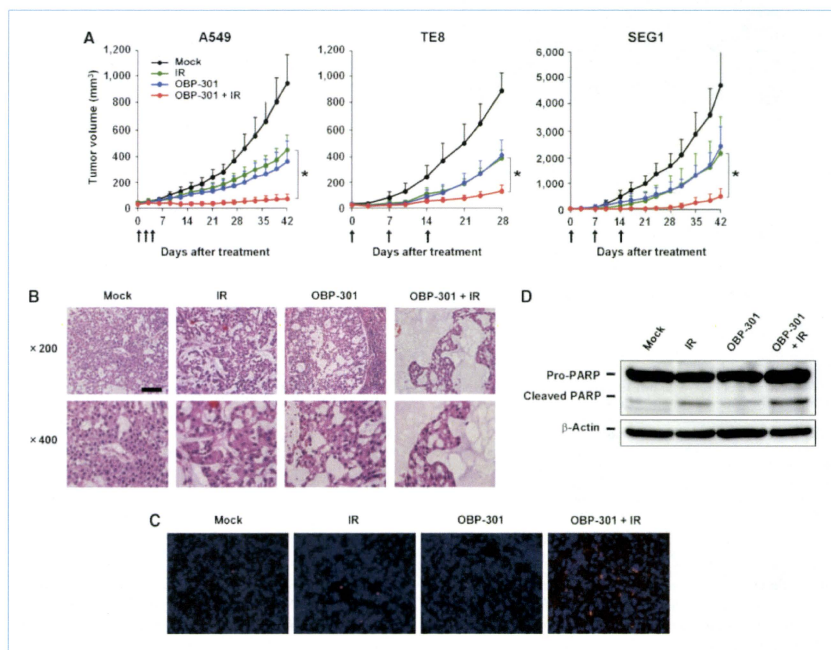


**Figure 4.** Antitumor effects of OBP-301 and ionizing radiation against s.c. established xenograft tumors. **A**, Cells ( $2 \times 10^6$  per mouse) were injected s.c. into the right flanks of mice. When the tumors reached 3 to 5 mm in diameter, mice were exposed to 3 Gy (for A549) or 2 Gy (for TE8 and SEG1) of ionizing radiation and intratumorally administered OBP-301 ( $1 \times 10^8$  PFU/tumor) for three cycles every 2 d (for A549) or every week (for TE8 and SEG1). Six (for A549) or eight (for TE8 and SEG1) mice were used for each group. Tumor growth is expressed as the mean tumor volume  $\pm$  SD. Arrows indicate each treatment. \*,  $P < 0.01$ . **B**, Mice bearing A549 xenografts were treated as described above. Tumor sections were obtained 10 d after the final administration of OBP-301. Paraffin sections of tumors were stained with hematoxylin and eosin. Scale bar, 100  $\mu$ m. Magnification,  $\times 200$  (top),  $\times 400$  (bottom). **C** and **D**, *In vivo* induction of apoptotic cell death by OBP-301 and ionizing radiation. **C**, paraffin-embedded sections of A549 subcutaneous tumors excised 3 d after treatment as described above were subjected to TUNEL staining. **D**, Western blot analysis for PARP and  $\beta$ -actin was done with proteins extracted from A549 subcutaneous tumors 3 d after treatments.

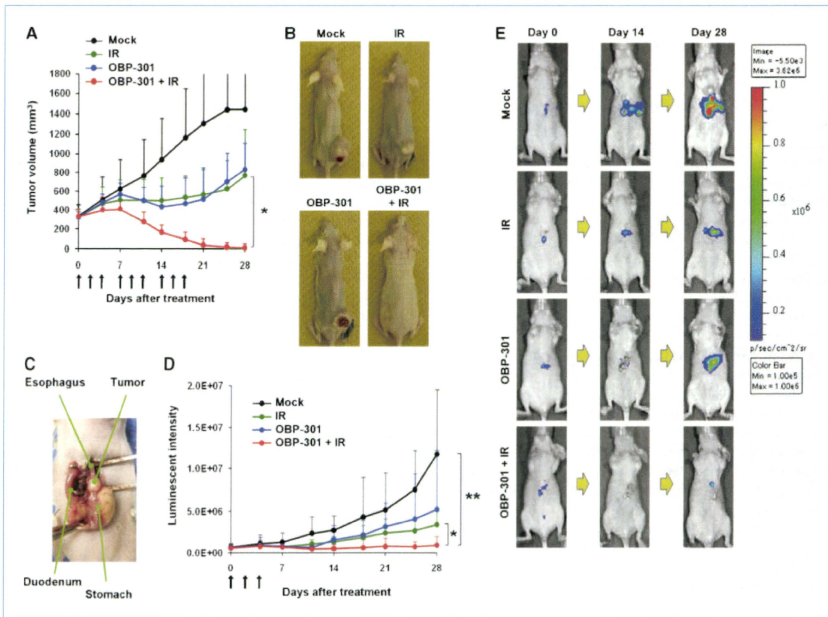


**Figure 5.** *In vivo* antitumor effects of OBP-301 and ionizing radiation against TE8 human esophageal cancer xenografts. **A**, larger subcutaneous TE8 tumors with a diameter of 8 to 10 mm were treated with OBP-301 followed by ionizing radiation three times per week (every 2 d) for three cycles (nine times in total). Ten mice were used for each group. Tumor growth is expressed as mean tumor volume  $\pm$  SD. Arrows indicate each treatment. \*,  $P < 0.01$ . **B**, macroscopic appearance of representative tumors 28 d after treatment. **C**, macroscopic appearance of orthotopic TE8-Luc esophageal tumor 3 wk after tumor cell inoculation ( $2 \times 10^6$  cells per mouse). **D**, mice bearing orthotopic TE8-Luc tumors were exposed to 2 Gy of ionizing radiation and intratumorally administered OBP-301 ( $1 \times 10^8$  PFU/tumor) for three cycles every 2 d. The luminescent intensity was measured by the IVIS imaging system 10 to 30 min after peritoneal administration of luciferin. Tumor growth is expressed by the luminescent intensity  $\pm$  SD. Arrows indicate each treatment. \*,  $P < 0.01$ ; \*\*,  $P < 0.05$ . **E**, representative images of mice treated with either ionizing radiation, OBP-301, or both on days 0, 14, and 28.

DNA repair can enhance the sensitivity of human tumor cells to ionizing radiation. The ATM activation by the MRN complex is essential for sensing and signaling from DNA DSBs and plays an important role in DNA repair and checkpoints, indicating that this pathway may be a good target for enhancing the antitumor effects of DNA-damaging agents. Indeed, ATM inhibitors, such as KU55933 and CGK733, and an MRN complex inhibitor, mirin, could sensitize cancer cells to therapeutic agents that cause DNA DSBs (21–23). Hsp90 interacts with the MRN complex, and an Hsp90 inhibitor enhances the sensitivity of tumor cells to radiation (24). Molecular disruption of MRN function by a dominant-negative mutant *Rad50* gene transfer sensitizes tumor cells to cisplatin (25). Although these approaches are effective in interrupting cellular DNA repair mechanisms, they lack tumor selectivity and may damage normal tissues when combined with DNA-

damaging therapies. Our data show that OBP-301 could synergize with ionizing radiation only in tumor cells but not in normal cells due to its telomerase dependency, suggesting that the regional administration of OBP-301 enables targeted radiosensitization.

The adenovirus *E1B* gene encodes a 19-kDa polypeptide (*E1B19kDa*) and a 55-kDa protein (*E1B55kDa*). The E1B55kDa protein induces a cellular environment conducive for viral protein synthesis via a complex with the E4orf6 protein (26). This E1B55kDa/E4orf6 complex degrades the MRN complex, blocks the downstream ATM signaling, and leads to a defective G<sub>2</sub>-M checkpoint in response to DSBs (10). Although the impact of E1B55kDa-mediated disruption of the MRN-ATM pathway on the DNA damage responses triggered by ionizing radiation has not yet been studied, we showed that OBP-301-mediated E1B55kDa expression induced the degradation of all components of the MRN



complex, which in turn prevented ATM autophosphorylation following ionizing radiation. OBP-301 expresses the *E1B* gene under the control of the hTERT promoter through an internal ribosome entry site sequence, whereas dl1520 (Onyx-015, CI-1042), which has been used in many clinical trials, was genetically modified by disruption of the coding sequence of the E1B55kDa protein (19). Therefore, ionizing radiation-induced ATM activation was blocked more efficiently by OBP-301 than by dl1520, which lacks E1B55kDa, although dl1520 slightly inhibited ATM phosphorylation, presumably due to E4orf6 protein expression (27).

One hallmark of DNA DSBs is the phosphorylation of H2AX at Ser139, a specialized histone H2A variant (referred to as  $\gamma$ H2AX; ref. 28); the reduction in  $\gamma$ H2AX levels in irradiated cells correlates with the repair of DSBs (29). OBP-301 infection apparently sustained the elevated levels of  $\gamma$ H2AX longer in irradiated tumor cells, indicating that tumor cells infected with OBP-301 could be rendered sensitive to ionizing radiation. We previously found that the process of oncolysis is morphologically distinct from apoptosis and necrosis, although autophagy is partially involved in this effect (30). The observation that OBP-301 infection significantly enhanced the induction of apoptosis when combined with ionizing radiation suggests that the radiosensitizing activity of OBP-301 is independent of virus-mediated oncolysis. Indeed, dephosphorylation of H2AX is associated with efficient DNA repair, whereas a pronounced increase in H2AX phosphorylation correlates with apoptosis (31, 32). Moreover, synergistically enhanced apoptosis by OBP-310 and ionizing radiation is likely to be p53 independent because p53 was ubiquitinated and degraded by E1B55kDa and E4orf6 proteins (16, 18).

Our *in vitro* studies suggest that OBP-301 infection and ionizing radiation may mutually sensitize human tumor cells, potentially leading to an effective combination treatment. OBP-301 infection requires a period of replication to induce the cytopathic effect and to sensitize cells to radiation, whereas ionizing radiation immediately causes DNA DSBs. Therefore, in a true clinical setting, multiple cycles of the external-beam radiotherapy followed by intratumoral injection of OBP-301 may yield optimal results. We confirmed the synergistic antitumor effect of three cycles of treatment with OBP-301 plus regional radiation and the *in vivo* induction of apoptotic cell death on subcutaneous human tumor xenografts. The orthotopic implantation of tumor cells, however, restores the correct tumor-host interactions, which do not occur when tumors are implanted in ectopic subcutaneous sites (33). Thus, we also showed the significant synergy of combined treatments in an orthotopic mouse model of human esophageal cancer by using a noninvasive whole-body imaging system.

There are some possible advantages of combining virotherapy with radiotherapy *in vivo*. First, OBP-301 may inhibit the vascular supply by killing endothelial cells because endothelial cell proliferation is increased in irradiated tumors (34), presumably with high telomerase activity. Alternatively, local irradiation itself may attack the vascular endothelial cells in the tumor site, which in turn can block the escape of locally injected OBP-301 into the blood circulation. Indeed, ionizing radiation inhibits endothelial cell prolifera-

tion, tube formation, migration, and clonogenic survival (35). Furthermore, in an immunocompetent environment, as we previously reported (36), OBP-301 stimulates host immune cells to produce endogenous antiangiogenic factors such as interferon- $\gamma$ . Second, virotherapy and radiotherapy may target tumor cells in different parts of tumors with distinct mechanisms. For example, tumor hypoxia has been considered a potential therapeutic problem because it renders tumor cells more resistant to ionizing radiation (37) and, therefore, some cells in certain parts of tumors may survive and proliferate under hypoxic conditions. In contrast, because hypoxia induces the transcriptional activity of hTERT gene promoter through hypoxia-inducible factor 1 $\alpha$  (38), OBP-301 can be expected to replicate and efficiently kill tumor cells even under hypoxic conditions. Thus, hTERT-specific oncolytic virotherapy can be effective in eliminating tumor cells that survive after local radiotherapy.

Another advantage of this combination therapy is that the area where each treatment shows the therapeutic effect is overlapping. The treatment field of radiotherapy includes primary tumors and regional lymph nodes. We previously showed that intratumorally injected OBP-301 expressing the *GFP* gene is effectively transported into the lymphatic circulation; viral replication produced GFP fluorescence signals in the metastatic lymph nodes in orthotopic human colorectal and oral cancer xenograft models (39, 40). Therefore, we anticipate that intratumoral OBP-301 administration will radiosensitize both primary tumors and regional lymph nodes.

In summary, our data show the molecular basis of radiosensitization induced by telomerase-specific virotherapy, in which the adenoviral E1B55kDa protein inhibits the radiation-induced DNA repair machinery through the interruption of the MRN function. OBP-301 infection and ionizing radiation mutually modulate their respective biological effects and thereby potentiate each other, profoundly enhancing *in vivo* antitumor activity in an orthotopic mouse model.

## Disclosure of Potential Conflicts of Interest

Y. Urata is an employee of Oncolys BioPharma, Inc., the manufacturer of OBP-301 (Telomelysin). The other authors disclosed no potential conflicts of interest.

## Acknowledgments

We thank Dr. Frank McCormick (University of California at San Francisco Helen Diller Family Comprehensive Cancer Center) for supplying the E1B55kDa-defective adenovirus mutant dl1520 (Onyx-015), and Tomoko Sueshi and Mitsuko Yokota for their excellent technical support.

## Grant Support

Ministry of Education, Culture, Sports, Science, and Technology of Japan (Toshiyoshi Fujiwara) and Ministry of Health, Labour, and Welfare of Japan (Toshiyoshi Fujiwara).

The costs of publication of this article were defrayed in part by the payment of page charges. This article must therefore be hereby marked *advertisement* in accordance with 18 U.S.C. Section 1734 solely to indicate this fact.

Received 06/29/2010; revised 09/13/2010; accepted 09/17/2010; published OnlineFirst 11/02/2010.

## References

- Bertzen SM, Harari PM, Bernier J. Exploitable mechanisms for combining drugs with radiation: concepts, achievements and future directions. *Nat Clin Pract Oncol* 2007;4:172–80.
- Bradley KA, Pollack IF, Reid JM, et al. Moxetaxin gadolinium and involved field radiation therapy for intrinsic pontine glioma of childhood: a Children's Oncology Group phase I study. *Neuro Oncol* 2008;10:752–8.
- Hoskin P, Rojas A, Saunders M. Accelerated radiotherapy, carbogen, and nicotinamide (ARCON) in the treatment of advanced bladder cancer: mature results of a Phase II nonrandomized study. *Int J Radiat Oncol Biol Phys* 2009;73:1425–31.
- Kim CH, Park SJ, Lee SH. A targeted inhibition of DNA-dependent protein kinase sensitizes breast cancer cells following ionizing radiation. *J Pharmacol Exp Ther* 2002;303:753–9.
- Tang X, Hui ZG, Cui XL, Garg R, Kastan MB, Xu B. A novel ATM-dependent pathway regulates protein phosphatase 1 in response to DNA damage. *Mol Cell Biol* 2008;28:2559–66.
- Shiloh Y. Ataxia-telangiectasia and the Nijmegen breakage syndrome: related disorders but genes apart. *Annu Rev Genet* 1997;31:635–62.
- Petrini JH. The Mre11 complex and ATM: collaborating to navigate S phase. *Curr Opin Cell Biol* 2000;12:293–6.
- Sturgeon CM, Roberge M. G2 checkpoint kinase inhibitors exert their radiosensitizing effects prior to the G2/M transition. *Cycl Cell* 2007;6:572–5.
- D'Amours D, Jackson SP. The Mre11 complex: at the crossroads of DNA repair and checkpoint signaling. *Nat Rev Mol Cell Biol* 2002;3:317–27.
- Carson CT, Schwartz RA, Stracker TH, Lilley CE, Lee DV, Weitzman MD. The Mre11 complex is required for ATM activation and the G2/M checkpoint. *EMBO J* 2003;22:6610–20.
- Theunissen JW, Kaplan MI, Hunt PA, et al. Checkpoint failure and chromosomal instability without lymphomagenesis in Mre11 (ATLD1/ATLD1) mice. *Mol Cell* 2003;12:1511–23.
- Kawashima T, Kagawa S, Kobayashi N, et al. Telomerase-specific replication-selective virotherapy for human cancer. *Clin Cancer Res* 2004;10:285–92.
- Umeoka T, Kawashima T, Kagawa S, et al. Visualization of intrathoracically disseminated solid tumors in mice with optical imaging by telomerase-specific amplification of a transferred green fluorescent protein gene. *Cancer Res* 2004;64:8259–65.
- Taki M, Kagawa S, Nishizaki M, et al. Enhanced oncolysis by a tropism-modified telomerase-specific replication-selective adenoviral agent OBP-405 (Telomelysin-RGD). *Oncogene* 2005;24:3130–40.
- Hashimoto Y, Watanabe Y, Shirakiya Y, et al. Establishment of biological and pharmacokinetic assays of telomerase-specific replication-selective adenovirus. *Cancer Sci* 2008;99:385–90.
- Queredo E, Marcellus RC, Lai A, et al. Regulation of p53 levels by the E1B 55-kilodalton protein and E4orf6 in adenovirus-infected cells. *J Virol* 1997;71:3788–98.
- Stracker TH, Carson CT, Weitzman MD. Adenovirus oncoproteins inactivate the Mre11-50-NBS1 DNA repair complex. *Nature* 2002;418:348–52.
- Schwartz RA, Lakdawala SS, Eshleman HD, Russell MR, Carson CT, Weitzman MD. Distinct requirements of adenovirus E1b55K protein for degradation of cellular substrates. *J Virol* 2008;82:9043–55.
- Bischoff JR, Kim DH, Williams A, et al. An adenovirus mutant that replicates selectively in p53-deficient human tumor cells. *Science* 1996;274:373–6.
- Chou TC. Theoretical basis, experimental design, and computerized simulation of synergism and antagonism in drug combination studies. *Pharmacol Rev* 2006;58:621–81.
- Crescenzi E, Palumbo G, de BJ, Brady HJ. Ataxia telangiectasia mutated and p21CIP1 modulate cell survival of drug-induced senescent tumor cells: implications for chemotherapy. *Clin Cancer Res* 2008;14:1877–87.
- Cheng WH, Muffic D, Mufitoglu M, et al. WRN is required for ATM activation and the S-phase checkpoint in response to interstrand cross-link-induced DNA double-strand breaks. *Mol Biol Cell* 2008;19:3293–33.
- Dupre A, Boyer-Chatenet L, Sattler RM, et al. A forward chemical genetic screen reveals an inhibitor of the Mre11-50-Nbs1 complex. *Nat Chem Biol* 2008;4:119–25.
- Dote H, Burgan WE, Camphausen K, Tofilon PJ. Inhibition of hsp90 compromises the DNA damage response to radiation. *Cancer Res* 2006;66:9211–20.
- Abuzeid WM, Jiang X, Shi G, et al. Molecular disruption of RAD50 sensitizes human tumor cells to cisplatin-based chemotherapy. *J Clin Invest* 2009;119:1974–85.
- Blackford AN, Grand RJ. Adenovirus E1B 55-kilodalton protein: multiple roles in viral infection and cell transformation. *J Virol* 2009;83:4000–12.
- Hart LS, Yannone SM, Naczki C, et al. The adenovirus E4orf6 protein inhibits DNA double strand break repair and radiosensitizes human tumor cells in an E1B-55K-independent manner. *J Biol Chem* 2005;280:1474–81.
- Redon C, Pilch D, Rogakou E, Sedelnikova O, Newrock K, Bonner W. Histone H2A variants H2AX and H2AZ. *Curr Opin Genet Dev* 2002;12:162–9.
- Banath JP, Macphail SH, Olive PL. Radiation sensitivity, H2AX phosphorylation, and kinetics of repair of DNA strand breaks in irradiated cervical cancer cell lines. *Cancer Res* 2004;64:7144–9.
- Endo Y, Sakai R, Ouchi M, et al. Virus-mediated oncolysis induces danger signal and stimulates cytotoxic T-lymphocyte activity via proteasome activator upregulation. *Oncogene* 2008;27:2375–81.
- Ewald B, Sampath D, Plunkett W. H2AX phosphorylation marks gemcitabine-induced stalled replication forks and their collapse upon S-phase checkpoint atrogation. *Mol Cancer Ther* 2007;6:1239–48.
- Cook PJ, Ju BG, Telesse F, Wang X, Glass CK, Rosenfeld MG. Tyrosine dephosphorylation of H2AX modulates apoptosis and survival decisions. *Nature* 2009;458:591–6.
- Fidler IJ. Rationale and methods for the use of nude mice to study the biology and therapy of human cancer metastasis. *Cancer Metastasis Rev* 1986;5:29–49.
- Tsai JH, Makonnen S, Feldman M, Sehgal CM, Maity A, Lee WM. Ionizing radiation inhibits tumor neovascularization by inducing ineffective angiogenesis. *Cancer Biol Ther* 2005;4:1395–400.
- Abdollahi A, Lipson KE, Sckell A, et al. Combined therapy with direct and indirect angiogenesis inhibition results in enhanced antiangiogenic and antitumor effects. *Cancer Res* 2003;63:8890–8.
- Ikedo Y, Kojima T, Kuroda S, et al. A novel antiangiogenic effect for telomerase-specific virotherapy through host immune system. *J Immunol* 2009;182:1763–9.
- Hockel M, Vaupel P. Tumor hypoxia: definitions and current clinical, biologic, and molecular aspects. *J Natl Cancer Inst* 2001;93:266–76.
- Nishi H, Nakada T, Kyo S, Inoue M, Shay JW, Isaka K. Hypoxia-inducible factor 1 mediates upregulation of telomerase (hTERT). *Mol Cell Biol* 2004;24:6076–83.
- Kishimoto H, Kojima T, Watanabe Y, et al. *In vivo* imaging of lymph node metastasis with telomerase-specific replication-selective adenovirus. *Nat Med* 2006;12:1213–9.
- Kurihara Y, Watanabe Y, Onimatsu H, et al. Telomerase-specific virotherapeutics for human head and neck cancer. *Clin Cancer Res* 2009;15:2335–43.

## Preclinical Evaluation of Telomerase-Specific Oncolytic Virotherapy for Human Bone and Soft Tissue Sarcomas

Tsuyoshi Sasaki<sup>1</sup>, Hiroshi Tazawa<sup>2,3</sup>, Jo Hasei<sup>1</sup>, Toshiyuki Kunisada<sup>1,4</sup>, Aki Yoshida<sup>1</sup>, Yuuri Hashimoto<sup>3</sup>, Shuya Yano<sup>3</sup>, Ryosuke Yoshida<sup>3</sup>, Toshihiro Uno<sup>2,3</sup>, Shunsuke Kagawa<sup>2,3</sup>, Yuki Morimoto<sup>1</sup>, Yasuo Urata<sup>5</sup>, Toshifumi Ozaki<sup>1</sup>, and Toshiyoshi Fujiwara<sup>2,3</sup>

### Abstract

**Purpose:** Tumor-specific replication-selective oncolytic virotherapy is a promising antitumor therapy for induction of cell death in tumor cells but not of normal cells. We previously developed an oncolytic adenovirus, OBP-301, that kills human epithelial malignant cells in a telomerase-dependent manner. Recent evidence suggests that nonepithelial malignant cells, which have low telomerase activity, maintain telomere length through alternative lengthening of telomeres (ALT). However, it remains unclear whether OBP-301 is cytopathic for nonepithelial malignant cells. Here, we evaluated the antitumor effect of OBP-301 on human bone and soft tissue sarcoma cells.

**Experimental Design:** The cytopathic activity of OBP-301, coxsackie and adenovirus receptor (CAR) expression, and telomerase activity were examined in 10 bone (OST, U2OS, HOS, HuO9, MNNG/HOS, SaOS-2, NOS-2, NOS-10, NDSC-1, and OUMS-27) and in 4 soft tissue (CCS, NMS-2, SYO-1, and NMFH-1) sarcoma cell lines. OBP-301 antitumor effects were assessed using orthotopic tumor xenograft models. The fiber-modified OBP-301 (termed OBP-405) was used to confirm an antitumor effect on OBP-301-resistant sarcomas.

**Results:** OBP-301 was cytopathic for 12 sarcoma cell lines but not for the non-CAR-expressing OUMS-27 and NMFH-1 cells. Sensitivity to OBP-301 was dependent on CAR expression and not on telomerase activity. ALT-type sarcomas were also sensitive to OBP-301 because of upregulation of human telomerase reverse transcriptase (*hTERT*) mRNA following virus infection. Intratumoral injection of OBP-301 significantly suppressed the growth of OST and SYO-1 tumors. Furthermore, fiber-modified OBP-405 showed antitumor effects on OBP-301-resistant OUMS-27 and NMFH-1 cells.

**Conclusions:** A telomerase-specific oncolytic adenovirus is a promising antitumor reagent for the treatment of bone and soft tissue sarcomas. *Clin Cancer Res*; 17(7): 1828–38. ©2011 AACR.

### Introduction

Bone and soft tissue sarcomas are annually diagnosed in 13,230 patients in the United States (1). They are the third most common cancer in children and account for 15.4% of all childhood malignancies. Treatment of patients with

bone and soft tissue sarcomas requires a multidisciplinary approach that involves orthopedic oncologists, musculoskeletal radiologists and pathologists, radiation oncologists, medical and pediatric oncologists, and microvascular surgeons (2, 3). Despite major advances in the treatment of bone and soft tissue sarcomas, such as neoadjuvant and adjuvant multiagent chemotherapy and aggressive surgery, about one fourth of the patients show a poor response to conventional therapy, resulting in subsequent recurrence and leading to a poor prognosis (1). Therefore, the development of a novel therapeutic strategy is required to cure patients with bone and soft tissue sarcomas.

Recent advances in molecular biology have fostered remarkable insights into the molecular basis of neoplasia. More than 85% of all human cancers, but only a few normal somatic cells, show high telomerase activity (4–6). Telomerase activity has also been detected in 17% to 81% of bone and soft tissue sarcomas (7–10). Telomerase activation is considered to be a critical step in cancer development, and its activity is closely correlated with the expression of human telomerase reverse transcriptase

**Authors' Affiliations:** <sup>1</sup>Department of Orthopaedic Surgery, Okayama University Graduate School of Medicine, Dentistry and Pharmaceutical Sciences; <sup>2</sup>Center for Gene and Cell Therapy, Okayama University Hospital; Departments of <sup>3</sup>Gastroenterological Surgery and <sup>4</sup>Medical Materials for Musculoskeletal Reconstruction, Okayama University Graduate School of Medicine, Dentistry and Pharmaceutical Sciences, Okayama; and <sup>5</sup>Oncolys BioPharma, Inc., Tokyo, Japan

**Note:** Supplementary data for this article are available at Clinical Cancer Research Online (<http://clincancerres.aacrjournals.org>).

**Corresponding Author:** Toshiyoshi Fujiwara, Department of Gastroenterological Surgery, Okayama University Graduate School of Medicine, Dentistry and Pharmaceutical Sciences, 2-5-1 Shikata-cho, Kita-ku, Okayama 700-8558, Japan. Phone: 81-86-235-7257; Fax: 81-86-221-8775. E-mail: toshi\_f@md.okayama-u.ac.jp

doi: 10.1158/1078-0432.CCR-10-2066

©2011 American Association for Cancer Research.



### Translational Relevance

Bone and soft tissue sarcomas frequently occur in young children and show aggressive progression, resistance to conventional chemotherapy, and poor prognosis, indicating a requirement for novel antitumor therapy to improve the clinical outcome. Telomerase-specific replication-selective oncolytic virotherapy is emerging as a promising antitumor therapy. We developed an oncolytic adenovirus, OBP-301, that efficiently kills human epithelial malignant cells in a telomerase-dependent manner. However, alternative lengthening of telomeres (ALT)-type nonepithelial malignant cells show low telomerase activity, suggesting lower effectiveness of OBP-301 in these cells. Here, we showed that OBP-301 has antitumor effects on both non-ALT-type and ALT-type sarcoma cells through upregulation of human telomerase reverse transcriptase mRNA. Furthermore, coxsackie and adenovirus receptor-negative sarcoma cells were efficiently killed by fiber-modified OBP-301 (termed OBP-405) through virus-integrin binding. Thus, a telomerase-specific oncolytic adenovirus would greatly improve the clinical outcome of young patients with advanced sarcomas.

(*hTERT*; ref. 11). Recently, telomerase-specific replication-selective oncolytic virotherapy has emerged as a promising antitumor therapy for induction of tumor-specific cell death. We previously developed an oncolytic adenovirus, OBP-301, in which the *hTERT* promoter drives the expression of the *E1A* and *E1B* genes linked to an internal ribosome entry site (IRES; ref. 12). We determined that OBP-301 efficiently induced the selective killing of a variety of human malignant epithelial cells, such as colorectal, prostate, and non-small cell lung cancers, but not of normal cells (12, 13). Furthermore, a phase I clinical trial of OBP-301, which was conducted in the United States on patients with advanced solid tumors, indicated that OBP-301 is well tolerated by patients (14).

There are 2 known telomere-maintenance mechanisms in human malignant tumors (15, 16): telomerase activation (4–6) and telomerase-independent alternative lengthening of telomeres (ALT; ref. 17–19). The ALT-type mechanism is more prevalent in tumors arising from nonepithelial tissues than in those of epithelial origin (20, 21). Therefore, ALT-type nonepithelial malignant cells frequently show low telomerase activity, suggesting that they have a low sensitivity to OBP-301, which kills cancer cells in a telomerase-dependent manner. However, it remains to be determined whether OBP-301 can exert an antitumor effect on human nonepithelial and on epithelial malignancies.

Adenovirus infection is mainly mediated by interaction of the virus with the coxsackie and adenovirus receptor (CAR) expressed on host cells (22). Therefore, while CAR-expressing tumor cells are the main targets for oncolytic

adenoviruses, tumor cells that lack CAR can escape from being killed by oncolytic adenoviruses. It has been reported that CAR is frequently expressed in human cancers of various organs such as the brain (23), thyroid (24), esophagus (25), gastrointestinal tract (26), and ovary (27). Bone and soft tissue sarcomas also express CAR (28–30). However, some populations of tumor cells lack CAR expression, suggesting a requirement for the development of a novel antitumor therapy against CAR-negative tumor cells. We recently developed fiber-modified OBP-301 (termed OBP-405), which can bind to not only CAR but also integrin molecules ( $\alpha v \beta 3$  and  $\alpha v \beta 5$ ) and efficiently kill CAR-negative tumor cells (31).

In the present study, we first investigated the *in vitro* cytopathic efficacy of OBP-301 against 14 human bone and soft tissue sarcoma cells. Next, the relationship between the cytopathic activity of OBP-301, CAR expression, and telomerase activity in human sarcoma cells was assessed. The *in vivo* antitumor effect of OBP-301 was also confirmed using orthotopic animal models. Finally, the antitumor effect of OBP-405 against OBP-301-resistant sarcoma cells was evaluated *in vitro* and *in vivo*.

### Materials and Methods

#### Cell lines

The human osteosarcoma (HuO9; ref. 32), chondrosarcoma (OUMS-27; ref. 33), and synovial sarcoma (SYO-1; ref. 34) cell lines were previously established in our laboratory. The human osteosarcoma cell lines OST, HOS, and SaOS-2 were kindly provided by Dr. Satoru Kyo (Kanazawa University, Ishikawa, Japan). The human clear cell sarcoma cell line CCS was maintained in our laboratory. These cells were propagated as monolayer cultures in Dulbecco's modified Eagle's medium (DMEM). The human osteosarcoma cell line U2OS was obtained from the American Type Culture Collection (ATCC) and was grown in McCoy's 5a medium. The human osteosarcoma cell line MNNG/HOS was purchased from DS Pharma Biomedical and was maintained in Eagle's minimum essential medium containing 1% nonessential amino acids. The human osteosarcoma cell lines NOS-2 and NOS-10 (35), the human dedifferentiated chondrosarcoma cell line NDCS-1 (36), the human malignant peripheral nerve sheath cell line NMS-2 (37), and the human malignant fibrous histiocytoma cell line NMFH-1 (38) were kindly provided by Dr. Hiroyuki Kawashima (Niigata University, Niigata, Japan) and were grown in RPMI-1640 medium. The transformed embryonic kidney cell line 293 was obtained from the ATCC and maintained in DMEM. All media were supplemented with 10% heat-inactivated FBS, 100 units/mL penicillin, and 100  $\mu$ g/mL streptomycin. The cells were maintained at 37°C in a humidified atmosphere with 5% CO<sub>2</sub>.

#### Recombinant adenoviruses

The recombinant tumor-specific, replication-selective adenovirus OBP-301 (Telomelysin), in which the promoter



element of the *hTERT* gene drives the expression of *E1A* and *E1B* genes linked with an IRES, was previously constructed and characterized (12, 13). OBP-405 is a telomerase-specific replication-competent adenovirus variant that was previously generated to express the RGD peptide in the fiber knob of OBP-301 (31). The *E1A*-deleted adenovirus vector dl312 and wild-type adenovirus serotype 5 (Ad5) were used as the control vectors. Recombinant viruses were purified by ultracentrifugation using cesium chloride step gradients, and their titers were determined by a plaque-forming assay by using 293 cells and they were stored at  $-80^{\circ}\text{C}$ .

#### Cell viability assay

Cells were seeded on 96-well plates at a density of  $1 \times 10^3$  cells/well 20 hours before viral infection. All cell lines were infected with OBP-301 or OBP-405 at multiplicity of infections (MOI) of 0, 0.1, 1, 10, 50, or 100 plaque forming units (PFU)/cell. Cell viability was determined on days 1, 2, 3, and 5 after virus infection, using a Cell Proliferation kit II (Roche Molecular Biochemicals) that was based on an XTT, sodium 3'-[1-(phenylaminocarbonyl)-3,4-tetrazolium]-bis(4-methoxy-6-nitro)benzene sulfonic acid hydrate, assay, according to the manufacturer's protocol. The  $\text{ID}_{50}$  value of OBP-301 for each cell line was calculated using cell viability data obtained on day 5 after virus infection.

#### Flow cytometric analysis

The cells ( $5 \times 10^5$ ) were labeled with mouse monoclonal anti-CAR (RmcB; Upstate Biotechnology), anti-human integrin  $\alpha\beta 3$  (LM609; Chemicon International), or anti-human integrin  $\alpha\beta 5$  (P1F6; Chemicon International) antibody for 30 minutes at  $4^{\circ}\text{C}$ . The cells were then incubated with fluorescein isothiocyanate (FITC)-conjugated rabbit anti-mouse IgG second antibody (Zymed Laboratories) and were analyzed using flow cytometry (FACS Array; Becton Dickinson). The mean fluorescence intensity (MFI) of CAR and integrin  $\alpha\beta 3$  or  $\alpha\beta 5$  for each cell line was determined by calculating the difference between the MFI in antibody-treated and nontreated cells from 3 independent experiments.

#### Quantitative real-time PCR analysis

U2OS cells, seeded on 6-well plates at a density of  $5 \times 10^5$  cells/well 20 hours before viral infection, were infected with Ad5, OBP-301, or dl312 at an MOI of 10 or 100 PFUs/cell. Mock-infected cells were used as controls. Furthermore, to confirm the modulation of *hTERT* mRNA expression by OBP-301 infection, CAR-positive and *hTERT* mRNA-expressing human sarcoma cell lines were seeded on 6-well plates at a density of  $5 \times 10^4$  cells/well 20 hours before viral infection and were infected with OBP-301 at an MOI of 100 PFUs/cell. Total RNA was extracted from the cells 2 days after virus infection by using the RNA-Bee reagent (Tel-Test Inc.). After synthesis of cDNA from 100 ng of total RNA, the levels of *hTERT* and glyceraldehyde-3-phosphate dehydrogenase (*GAPDH*) mRNA expression were determined using quantitative real-time PCR and a Step One Plus Real Time PCR System (Applied Biosystems) and TaqMan Gene

Expression Assays (Applied Biosystems). The relative levels of *hTERT* mRNA expression were calculated by using the  $2^{-\Delta\Delta\text{Ct}}$  method (39) after normalization with reference to the expression of *GAPDH* mRNA.

To compare the *E1A* copy number between OBP-301- and Ad5-infected U2OS cells, U2OS cells, seeded on 6-well plates at a density of  $5 \times 10^5$  cells/well 20 hours before viral infection, were infected with OBP-301 or Ad5 at an MOI of 10 PFUs/cell. Genomic DNA was extracted from serially diluted viral stocks, and tumor cells were infected with OBP-301 or Ad5 by using the QIAmp DNA Mini Kit (Qiagen). *E1A* copy number was also determined using TaqMan real-time PCR systems (Applied Biosystems).

#### *In vivo* OST and OUMS-27 xenograft tumor models

Animal experimental protocols were approved by the Ethics Review Committee for Animal Experimentation of Okayama University School of Medicine. The OST and OUMS-27 cells ( $5 \times 10^6$  cells per site) were inoculated into the tibia or the flank of female athymic nude mice aged 6 to 7 weeks (Charles River Laboratories). Palpable tumors developed within 14 to 21 days and were permitted to grow to approximately 5 to 6 mm in diameter. At that stage, a 50  $\mu\text{L}$  volume of solution containing OBP-301, OBP-405, dl312, or PBS was injected into the tumors. Tumor size was monitored by measuring tumor length and width by using calipers. The volumes of OUMS-27 tumors were calculated using the following formula:  $(L \times W^2) \times 0.5$ , where  $L$  is the length and  $W$  is the width of each tumor. The volumes of OST tumors were calculated using the formula:  $(L + W) \times L \times W \times 0.2618$ , as previously reported (40).

#### X-ray examination

The formation of osteolytic lesions was monitored using radiography (FUJIFILM IXFR film; FUJIFILM Co.) and an X-ray system (SOFTEX TYPE CMB; SOFTEX Co.).

#### Histopathologic analysis

Tumors were fixed in 10% neutralized formalin and embedded in paraffin blocks. Sections were stained with hematoxylin/eosin (H&E) and analyzed by light microscopy.

#### Statistical analysis

Data are expressed as means  $\pm$  SD. Student's  $t$  test was used to compare differences between groups. Pearson's product-moment correlation coefficients were calculated using PASW statistics version 18 software (SPSS Inc.). Statistical significance was defined when the  $P$  value was less than 0.05.

## Results

#### *In vitro* cytopathic efficacy of OBP-301 against human bone and soft tissue sarcoma cell lines

To evaluate the *in vitro* cytopathic effect of OBP-301 against nonepithelial malignant cells, 14 tumor cell lines

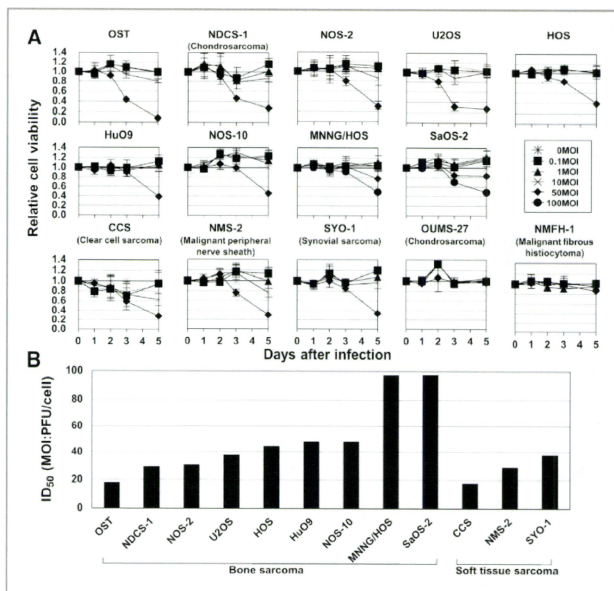


**Figure 1.** Cytopathic effect of OBP-301 on human bone and soft tissue sarcoma cell lines. A, cells were infected with OBP-301 at the indicated MOI, and cell survival was quantified over 5 days using the XTT assay. The cell viability of mock-treated group on each day was considered 1.0, and the relative cell viability was calculated. Data are means  $\pm$  SD. The types of tumor except for osteosarcoma were shown in parentheses. B, the 50% inhibiting doses of OBP-301 on cell viability 5 days after infection were calculated and are expressed as ID<sub>50</sub> values.

derived from human bone and soft tissue sarcomas were infected with various doses of OBP-301. The cell viability of each cell line was assessed over 5 days after infection by the XTT assay. OBP-301 infection induced cell death in a time-dependent manner in all sarcoma cell lines except for the OUMS-27 and NMFH-1 cell lines (Fig. 1A). Calculation of the ID<sub>50</sub> values revealed that, of the 12 OBP-301-sensitive sarcoma cell lines, MNNC/HOS and SaOS-2 cells were relatively less sensitive than the other 10 sarcoma cell lines (Fig. 1B). Furthermore, to rule out the possibility that cytopathic effect of OBP-301 is due to nonspecific toxicity based on the high uptake of virus particles into tumor cells, we examined the cytopathic activity of replication-deficient dl312 in U2OS and HOS cells. dl312 did not show any cytopathic effect in U2OS and HOS cells, even when these cells were infected with dl312 at high dose (50 and 100 MOIs; Supplementary Fig. S1). These results indicate that OBP-301 is cytopathic for most human bone and soft tissue sarcoma cell lines but that some sarcoma cell lines are resistant to OBP-301.

#### Expressions of the adenovirus receptor and *hTERT* mRNA on human bone and soft tissue sarcoma cell lines

Because adenovirus infection efficiency depends mainly on cellular CAR expression (22), we determined the expres-

sion level of CAR on the 14 sarcoma cell lines by flow cytometry. The 12 OBP-301-sensitive sarcoma cell lines showed CAR expression, determined as MFIs, at various levels, whereas the OBP-301-resistant OUMS-27 and NMFH-1 cells did not express CAR (Fig. 2A and Supplementary Fig. S2).

OBP-301 contains the *hTERT* gene promoter, which allows it to tumor specifically regulate the gene expression of *E1A* and *E1B* for viral replication. Thus, OBP-301 can efficiently replicate in human cancer cells with high telomerase activity but not in normal cells without telomerase activity (12). Recently, some populations of human sarcoma cells have been shown to possess low telomerase activity and to maintain telomere lengths through an ALT mechanism (17–19). Thus, it is probable that OBP-301 cannot efficiently replicate in, and kill, ALT-type human sarcoma cells because of their low telomerase activity. To assess whether the telomerase activity of human sarcoma cells affects the cytopathic activity of OBP-301, we analyzed *hTERT* mRNA expression levels in the 14 sarcoma cell lines by quantitative real-time reverse transcriptase PCR (RT-PCR) analysis. Thirteen of the sarcoma cell lines had detectable *hTERT* mRNA expression at variable levels, and only SaOS-2 cells did not express *hTERT* mRNA (Fig. 2B).



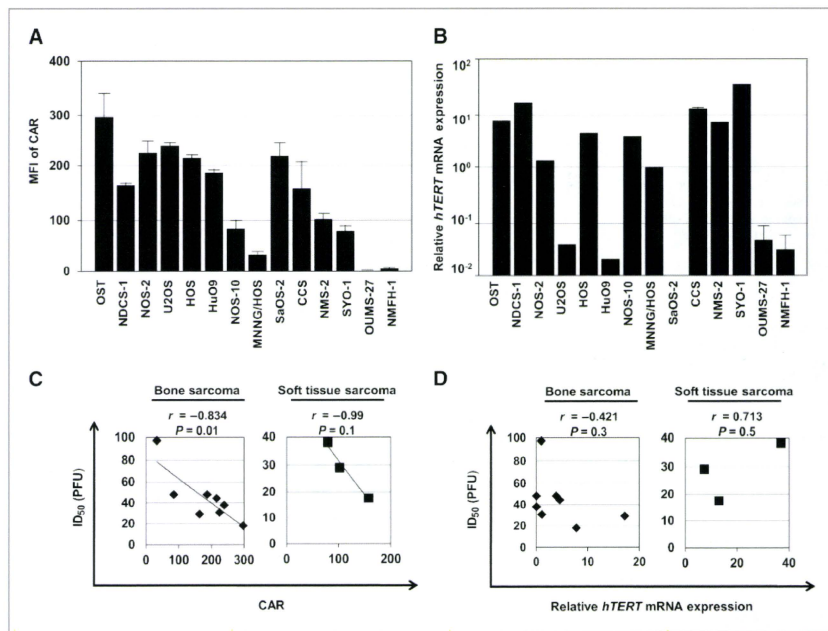


**Figure 2.** Relationship between the expression levels of CAR and *hTERT* mRNA and the cytopathic activity of OBP-301 against human bone and soft tissue sarcoma cell lines. A, the MFI of CAR expression on human bone and soft tissue sarcoma cells. The cells were incubated with a monoclonal anti-CAR (RmcB) antibody, followed by flow cytometric detection using a FITC-labeled secondary antibody. B, expression of *hTERT* mRNA in human bone and soft tissue sarcoma cells by quantitative real-time PCR. The relative levels of *hTERT* mRNA were calculated after normalization with reference to the expression of *GAPDH* mRNA. C, correlation between the MFI of CAR and the ID<sub>50</sub> of OBP-301 on human bone and soft tissue sarcoma cells. D, correlation between *hTERT* mRNA expression and the ID<sub>50</sub> of OBP-301 on human bone and soft tissue sarcoma cells. Statistical significance was determined as  $P < 0.05$ , after analysis of Pearson's correlation coefficient.

We next investigated the relationship between CAR and *hTERT* mRNA expressions and the cytopathic activity of OBP-301 among the 11 CAR-positive sarcoma cell lines with *hTERT* gene expression. CAR expression levels significantly ( $r = -0.834$ ;  $P = 0.01$ ) correlated with the cytopathic activity of OBP-301 against 8 of the bone sarcoma cell lines (Fig. 2C). CAR expression in 3 of the soft tissue sarcoma cell lines also correlated ( $r = -0.99$ ) with the cytopathic effect of OBP-301, but the differences did not reach significance ( $P = 0.1$ ) because of the low number of cell lines assayed. In contrast, there was no significant correlation between *hTERT* mRNA expression and the cytopathic activity of OBP-301 (Fig. 2D). These results indicate that the cytopathic activity of OBP-301, at least in part, depends on CAR expression.

Furthermore, SaOS-2 and U2OS cells have already been shown to be ALT-type sarcoma cell lines with low telomer-

ase activity (9, 17). Among these ALT-type sarcoma cells, U2OS cells showed a sensitivity to OBP-301 that was similar to that of non-ALT-type sarcoma cells such as HOS and NOS-10 (Fig. 1B). These results indicate that ALT-type human sarcoma cells are sensitive to OBP-301 and that a low telomerase activity does not detract from the cytopathic activity of OBP-301.

#### Enhanced virus replication and cytopathic activity of OBP-301 through *hTERT* mRNA upregulation in ALT-type sarcoma cell lines

The high sensitivity of ALT-type sarcoma cells to OBP-301 prompted us to hypothesize that OBP-301 may activate the *hTERT* gene promoter, thereby enhancing the viral replication rate and subsequently inducing cytopathic activity in ALT-type sarcoma cells. Furthermore, it has been previously shown that the adenoviral E1A

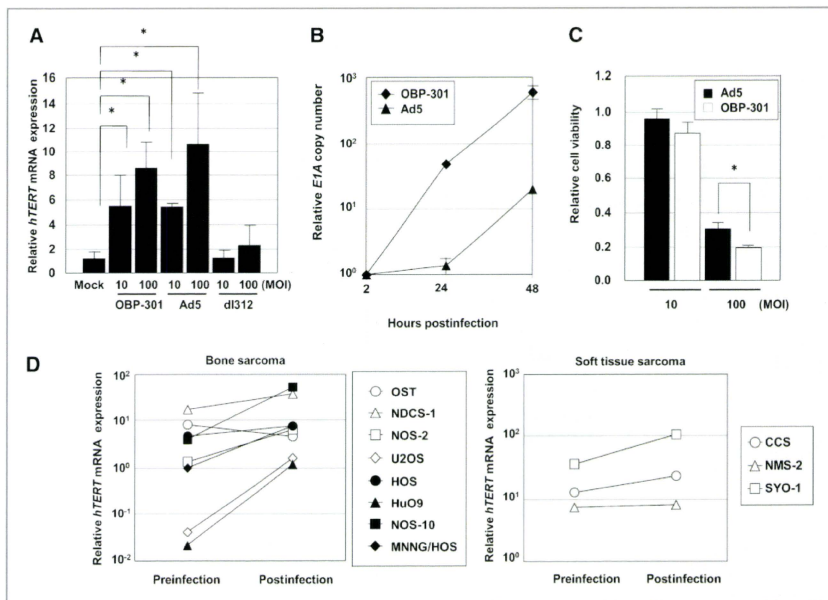


**Figure 3.** Upregulation of *hTERT* gene expression in ALT-type human sarcoma cell lines enhances the replication and the cytopathic effect of OBP-301. **A**, expression of *hTERT* mRNA in U2OS cells that were mock-infected or were infected with OBP-301, Ad5, or dl312 at the indicated MOIs for 48 hours, and *hTERT* mRNA expression was analyzed using quantitative real-time RT-PCR. The value of *hTERT* mRNA expression in the mock-infected cells was set at 1, and relative mRNA levels were plotted. **B**, quantitative measurement of viral DNA replication in U2OS cells infected with OBP-301 or Ad5. The cells were infected with OBP-301 or Ad5 at an MOI of 10 PFUs/cell, and *E1A* copy number was analyzed over the following 2 days by quantitative real-time PCR. The value of the *E1A* copy number at 2 hours after infection was set at 1, and relative copy numbers were plotted. **C**, comparison of the cytopathic effect of OBP-301 and Ad5 in U2OS cells. The cells were infected with OBP-301 or Ad5 at the indicated MOIs, and cell survival was quantified 5 days after infection by using an XTT assay. **D**, expression of *hTERT* mRNA after infection of human bone (left) and soft tissue (right) sarcoma cell lines with OBP-301 at an MOI of 100 PFUs/cell. Statistical significance (\*) was determined as  $P < 0.05$  (Student's *t* test).

protein can activate the promoter activity of the *hTERT* gene (41, 42). Therefore, to determine whether OBP-301 infection activates *hTERT* mRNA expression, we examined the expression level of *hTERT* mRNA in ALT-type U2OS cells after infection with OBP-301 at MOIs of 10 and 100 PFUs/cell (Fig. 3A). Compared with mock-infected U2OS cells, OBP-301-infected U2OS cells showed a 6- to 8-fold increase in *hTERT* mRNA expression in a dose-dependent manner. Ad5 infection also increased *hTERT* mRNA expression in U2OS cells, whereas there was no increase in U2OS cells infected with *E1A*-deleted dl312. These results suggest that OBP-301 is cytopathic for ALT-type sarcoma cells through *E1A*-mediated activation of the *hTERT* gene promoter.

We next compared viral replication rates after infection of ALT-type U2OS cells with OBP-301 or Ad5. As expected, the viral replication rate of OBP-301 was significantly

higher than that of Ad5 (Fig. 3B). Furthermore, the cytopathic activity of OBP-301 was significantly higher than that of Ad5 against the ALT-type U2OS cells (Fig. 3C). Finally, to determine whether OBP-301 activates *hTERT* mRNA expression in both ALT-type and non-ALT-type human sarcoma cell lines, we infected 11 CAR-positive human sarcoma cells with OBP-301 at 100 MOI. Ten of the 11 CAR-positive human sarcoma cell lines showed an increase in the expression level of *hTERT* mRNA after OBP-301 infection that ranged from a 1.1- to 50.0-fold increase (Fig. 3D and Supplementary Table S1). In addition, the expression level of *hTERT* mRNA was also upregulated when OST cells were infected with 5 or 50 MOI of OBP-301 (Supplementary Fig. S3). These results suggest that OBP-301 is cytopathic for both ALT-type and non-ALT-type human sarcoma cells through activation of the *hTERT* gene promoter.



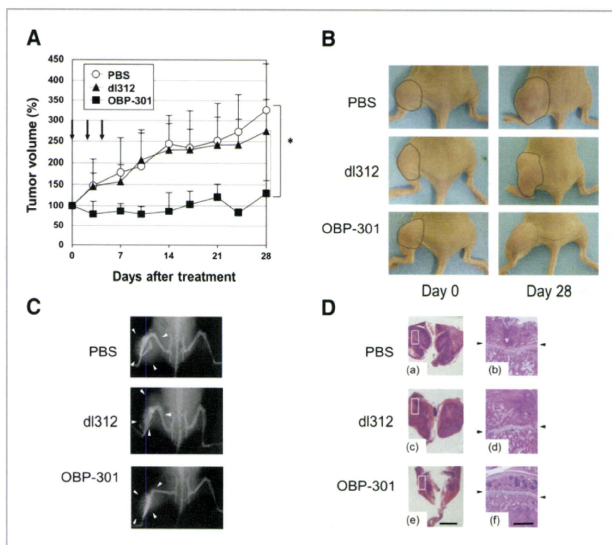


**Figure 4.** Antitumor effect of OBP-301 in an orthotopic OST bone sarcoma xenograft model. **A**, athymic nude mice were inoculated intratibially with OST cells ( $5 \times 10^6$  cells/site). Fourteen days after inoculation (designated as day 0), OBP-301 (■) or OBP-405 (▲) was injected into the tumor, with  $1 \times 10^8$  PFUs on days 0, 2, and 4. PBS (○) was used as a control. Four mice were used for each group. Tumor growth was expressed as mean tumor volume  $\pm$  SD. Statistical significance (\*) was determined as  $P < 0.05$  (Student's *t* test). **B**, macroscopic appearance of OST tumors in nude mice on days 0 and 28 after treatment with PBS, dl312, or OBP-301. Tumor masses are outlined by a dotted line. **C**, X-ray photographs of mice bearing OST tumors. The white arrowheads indicate the space occupied by the tumor mass. **D**, histologic analysis of the OST tumors. Tumor sections were obtained 28 days after inoculation of tumor cells. Paraffin-embedded sections of OST tumors were stained with H&E. The black arrowheads indicate growth plate cartilages. a, c and e, are low-magnification images and b, d and f are high-magnification images of the area outlined by a white square. Left scale bar, 5 mm. Right scale bar, 500  $\mu$ m.

#### Antitumor effect of OBP-301 against 2 orthotopic tumor xenograft models

To evaluate the *in vivo* antitumor effect of OBP-301 against human bone and soft tissue sarcomas, we used 2 types of orthotopic tumor xenograft models: the OST bone sarcoma xenograft and the SYO-1 subcutaneous soft tissue sarcoma xenograft. We first identified a dose of OBP-301 that was suitable for induction of an antitumor effect in the subcutaneous OST bone sarcoma xenograft model (determined as  $>10^7$  PFUs; Supplementary Fig. S4). We next assessed the antitumor effect of OBP-301 on the orthotopic OST bone sarcoma xenograft model. OBP-301 was injected into the tumor once a day for 3 days, with  $10^8$  PFUs per day (10). Replication-deficient adenovirus dl312 or PBS was also injected into control groups. Tumor growth was significantly suppressed by OBP-301 injection compared with injection of dl312 or PBS (Fig. 4A). Macroscopic analysis of the tumors indicated that OBP-301-treated tumors were consistently smaller than dl312- or PBS-treated tumors on day 28 after treatment (Fig 4B). We further determined whether OBP-301-

treated tumors were less destructive to surrounding normal tissues than control tumors, using X-ray and histologic analyses (Fig. 4C and D). X-ray examination revealed that OBP-301-treated tumors resulted in less bone destruction than dl312- or PBS-treated tumors. Histologic findings were consistent with the X-ray results, showing that some tumor tissue had penetrated over the growth plate cartilage in dl312- and PBS-treated tumors but not in OBP-301-treated tumors.

With future clinical application in mind, we sought to establish a suitable protocol for repeated intratumoral injection of OBP-301 by using an orthotopic SYO-1 soft tissue sarcoma xenograft model. Doses of OBP-301 that were suitable for induction of an antitumor effect on SYO-1 tumors ( $>10^8$  PFUs) were determined in a manner similar to that of OST bone sarcoma cells (data not shown). OBP-301 was injected 3 times into the tumor, with  $10^8$  PFUs and intervals of 1 day, 2 days, or 1 week between injections (Supplementary Fig. S5). A total of 3 OBP-301 injections, with intervals of 2 days or 1 week between injections, induced a significant

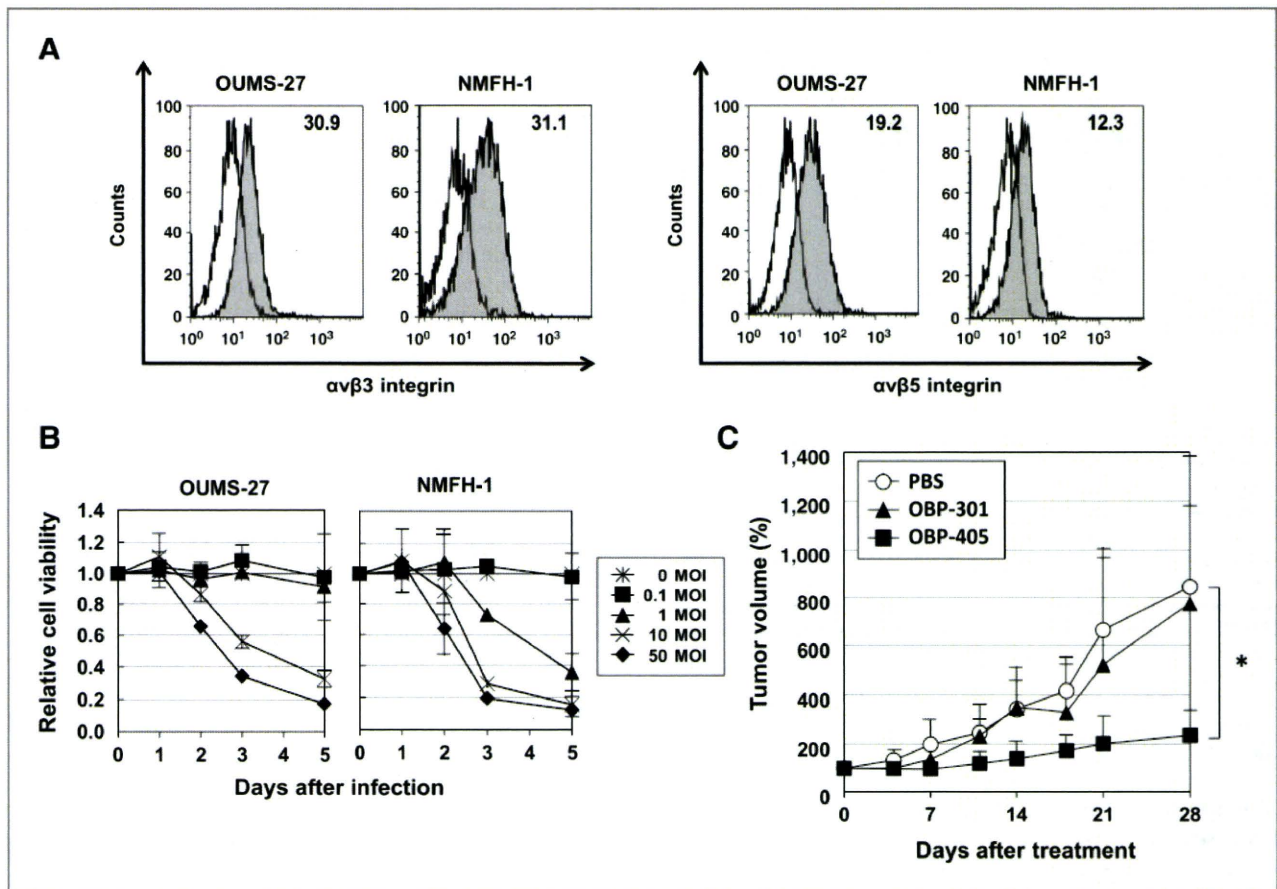


Figure 5. *In vitro* and *in vivo* antitumor effects of OBP-405 on OBP-301-resistant human sarcoma cell lines. A, expression of the integrins  $\alpha v \beta 3$  (left) and  $\alpha v \beta 5$  (right) on OUMS-27 and NMFH-1 cells. The cells were incubated with a monoclonal anti- $\alpha v \beta 3$  integrin (LM609) or an anti- $\alpha v \beta 5$  integrin (P1F6), followed by flow cytometric detection using an FITC-labeled secondary antibody. The gray histogram represents integrin antibody staining. The number at the top right-hand corner of each graph is the MFI. B, cytopathic effect of OBP-405 on OUMS-27 and NMFH-1 cells. The cells were infected with OBP-405 at the indicated MOI values, and cell survival over 5 days was quantified using an XTT assay. C, antitumor effect of OBP-405 in a subcutaneous OUMS-27 xenograft tumor model. Athymic nude mice were inoculated subcutaneously with OUMS-27 cells ( $5 \times 10^6$  cells/site). Fourteen days after inoculation (designated as day 0), OBP-301 ( $\blacktriangle$ ) or OBP-405 ( $\blacksquare$ ) was injected into the tumor, with  $1 \times 10^8$  PFUs on days 0, 2, and 4. PBS ( $\circ$ ) was used as a control. Ten mice were used for each group. Tumor growth was expressed as the mean tumor volume  $\pm$  SD. Statistical significance (\*) was determined as  $P < 0.05$  (Student's *t* test).

suppression of tumor growth, whereas intervals of 1 day between injections were not effective. These results suggest that an interval of more than 2 days between injections is necessary to efficiently suppress tumor growth by repeated injections of OBP-301.

#### Antitumor effect of OBP-405 on OBP-301-resistant sarcoma cell lines

OUMS-27 and NMFH-1 cells are resistant to OBP-301 because they lack CAR expression (Fig. 1A and Supplementary Fig. S2). We previously developed a fiber-modified OBP-301, termed OBP-405, which can enter not only CAR-positive cancer cells but also CAR-negative cancer cells through binding to the cell surface integrins  $\alpha v \beta 3$  and  $\alpha v \beta 5$  (31). We therefore sought to evaluate the antitumor effect of OBP-405 on the OBP-301-resistant OUMS-27 and NMFH-1 cells. We first examined the expression levels of

the integrins  $\alpha v \beta 3$  and  $\alpha v \beta 5$  on the surface of these cells by flow cytometry (Fig. 5A). OUMS-27 and NMFH-1 cells expressed both integrin molecules. We next examined the effect of OBP-405 on OUMS-27 and NMFH-1 cell viability by using the XTT assay (Fig. 5B). OBP-405 efficiently suppressed cell viability of both of these cell lines in a dose- and time-dependent manner. We further assessed whether OBP-405 has an *in vivo* antitumor effect by assaying the effect of 3 intratumoral injections of OBP-301 or OBP-405, with  $10^8$  PFUs or of control PBS, into subcutaneous OUMS-27 tumor xenografts. As shown in Figure 5C, administration of OBP-405 resulted in significant suppression of tumor growth compared with OBP-301- or PBS-treated tumors 28 days after treatment. These results suggest that fiber-modified OBP-405 is a potential antitumor reagent that is effective against CAR-negative human sarcoma cells.



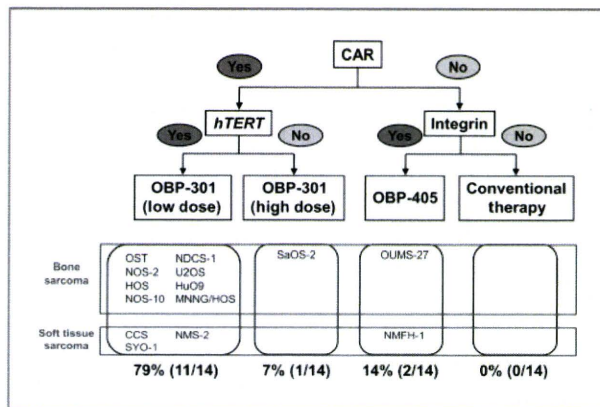


Figure 6. Outline of a therapeutic strategy for the use of telomerase-specific replication-selective oncolytic adenoviruses for human bone and soft tissue sarcoma cells. Assessment of CAR expression in tumor cells could serve as an indicator for OBP-301 or OBP-405 treatment. Of the 14 human sarcoma cell lines shown, the 12 CAR-expressing sarcoma cells (86%) should be treated with OBP-301 and the 2 sarcoma cells (14%) that lack CAR expression should be treated with OBP-405. The tumor expression level of *hTERT* mRNA would be useful in deciding the dose of OBP-301 to be used for treatment. The expression level of integrins on the tumor surface should be confirmed prior to OBP-405 treatment.

## Discussion

Telomerase-specific replication-selective oncolytic adenoviruses are emerging as promising antitumor reagents for induction of tumor-specific cell death. We previously reported that OBP-301 has a strong antitumor effect on a variety of human epithelial malignant cells that have high telomerase activity (12, 13). However, nonepithelial malignant cells often show low telomerase activity and instead maintain telomere length through an ALT mechanism (20, 21). The effect of OBP-301 on human bone and soft tissue sarcoma cells has not been extensively examined. In this study, we showed that OBP-301 induced cell death in 12 of 14 human bone and soft tissue sarcoma cell lines (Fig. 1) and that the cytopathic activity of OBP-301 significantly correlated with tumor CAR expression (Fig. 2A). Furthermore, 2 ALT-type sarcoma cells showed low *hTERT* mRNA expression (Fig. 2B) but a similar sensitivity to OBP-301 compared with non-ALT-type cells because of *hTERT* mRNA upregulation by OBP-301 infection (Fig. 3). In contrast, 2 OBP-301-resistant sarcoma cells that lack CAR expression were highly sensitive to OBP-405, which can infect cells by binding to surface integrin molecules (Fig. 5). On the basis of these results, and with future clinical application in mind, we established a therapeutic strategy for the use of telomerase-specific oncolytic adenoviruses to treat patients with bone and soft tissue sarcomas (Fig. 6). This strategy involves assessment of the expression levels of CAR, *hTERT*, and integrins on human sarcoma cells, which would then allow easy selection of the most effective protocol for the treatment of patients by using oncolytic adenoviruses. Furthermore, as OBP-301 and OBP-405 show

the profound antitumor effect in the combination of various chemotherapeutic agents (43, 44), further evaluation for the strategy using OBP-301 and OBP-405 in combination with chemotherapy should be warranted.

The cytopathic activity of OBP-301 significantly correlated with CAR expression, but not with telomerase activity, of human sarcoma cells (Fig. 2). These results suggest that the cytopathic activity of OBP-301 depends primarily on infection efficiency rather than virus replication. Primary epithelial and nonepithelial malignant tumors frequently express CAR (23–30). However, CAR expression can often be downregulated by tumor progression (45, 46) or under hypoxic conditions (47), possibly leading to a low infection efficiency and resistance to OBP-301. Thus, for future clinical application of OBP-301, it may be necessary to overcome the resistance to OBP-301 that arises during tumor progression. A histone deacetylase (HDAC) inhibitor has been previously shown to enhance CAR expression on human cancer cells (48–50). Therefore, for the treatment of OBP-301-resistant sarcomas, it may be necessary to either upregulate CAR expression on tumor cells in combination with an HDAC inhibitor or use OBP-405 to kill tumor cells in an integrin-dependent manner (31).

ALT-type sarcoma cells that express a low level of *hTERT* mRNA showed sensitivity to OBP-301 that was similar to that of non-ALT-type sarcoma cells (Figs. 1 and 2). We further showed that OBP-301 infection upregulates *hTERT* gene expression and subsequently activates virus replication and cytopathic activity in ALT-type sarcoma cells (Fig. 3). These results suggest that the *hTERT* gene promoter is a useful tool for enhancement of the oncolytic adenoviruses not only because it induces tumor-specific virus replication but also because it enhances virus replication after infection. Indeed, the ALT-type sarcoma SaOS-2 cells that lack *hTERT* gene expression were relatively less sensitive to OBP-301 than the other ALT-type sarcoma U2OS cells that express low levels of *hTERT* mRNA (Figs. 1 and 2). We further observed that *hTERT* mRNA expression was not upregulated after OBP-301 infection of SaOS-2 cells (data not shown). These results suggest that if *hTERT* gene expression cannot be detected in tumor cells, then ALT-type sarcoma cells should be treated with high doses of OBP-301, or with OBP-405, to enhance OBP-301 infection efficiency (Fig. 6).

It is also worth noting in terms of future clinical application that an interval of more than 2 days between injections is necessary in order for repeated injections of OBP-301 to induce a strong antitumor effect in an SYO-1 animal xenograft model (Supplementary Fig. S5). We first expected that continuous injection of OBP-301 at intervals of 1 day, when tumors are of a minimum size, might be more effective in inducing an antitumor effect than injection at intervals of 2 days or 1 week. Surprisingly, continuous injection of OBP-301 at intervals of 1 day, for 3 days, could not induce an antitumor effect. There are 2 possible explanations for these results. The



first possibility is that 3 days of continuous injections may not provide enough time for OBP-301 to replicate and reach the minimal dose required for induction of an antitumor effect within tumor tissues. The second possibility is that OBP-301 may be less effective against more slowly proliferating tumor cells than it is against rapidly proliferating tumor cells because its replication rate would be lower in the more slowly proliferating cells. Although it remains unclear why continuous injection of OBP-301 was less effective, it is clear that repeated infection with OBP-301 at intervals of more than 2 days would be sufficient to exert an antitumor effect against human sarcoma tissues.

In conclusion, we have clearly shown that OBP-301 has strong *in vitro* and *in vivo* antitumor effects against human bone and soft tissue sarcoma cells. Telomerase-specific replication-selective oncolytic virotherapy would provide a new platform for the treatment of patients with bone and soft tissue sarcomas.

## References

- Jemal A, Siegel R, Ward E, Hao Y, Xu J, Thun MJ. Cancer statistics, 2009. *CA Cancer J Clin* 2009;59:225-49.
- Gilbert NF, Cannon CP, Lin PP, Lewis VO. Soft-tissue sarcoma. *J Am Acad Orthop Surg* 2009;17:40-7.
- Weber K, Damron TA, Frassica FJ, Sim FH. Malignant bone tumors. *Instr Course Lect* 2008;57:673-88.
- Kim NW, Piatyszek MA, Prowse KR, Harley CB, West MD, Ho PL, et al. Specific association of human telomerase activity with immortal cells and cancer. *Science* 1994;266:2011-5.
- Shay JW, Wright WE. Telomerase activity in human cancer. *Curr Opin Oncol* 1996;8:66-71.
- Artandi SE, DePinho RA. Telomeres and telomerase in cancer. *Carcinogenesis* 2010;31:9-18.
- Aogi K, Woodman A, Urquidí V, Mangham DC, Tarin D, Goodison S. Telomerase activity in soft-tissue and bone sarcomas. *Clin Cancer Res* 2000;6:4776-81.
- Umehara N, Ozaki T, Sugihara S, Kunisada T, Morimoto Y, Kawai A, et al. Influence of telomerase activity on bone and soft tissue tumors. *J Cancer Res Clin Oncol* 2004;130:411-6.
- Terasaki T, Kyo S, Takakura M, Maida Y, Tsuchiya H, Tomita K, et al. Analysis of telomerase activity and telomere length in bone and soft tissue tumors. *Oncol Rep* 2004;11:1307.
- Yoo J, Robinson RA. Expression of telomerase activity and telomerase RNA in human soft tissue sarcomas. *Arch Pathol Lab Med* 2000;124:393-7.
- Nakayama J, Tahara H, Tahara E, Saito M, Ito K, Nakamura H, et al. Telomerase activation by hTERT in human normal fibroblasts and hepatocellular carcinomas. *Nat Genet* 1998;18:65-8.
- Kawashima T, Kagawa S, Kobayashi N, Shirakiya Y, Umeoka T, Teraishi F, et al. Telomerase-specific replication-selective virotherapy for human cancer. *Clin Cancer Res* 2004;10:285-92.
- Hashimoto Y, Watanabe Y, Shirakiya Y, Uno F, Kagawa S, Kawamura H, et al. Establishment of biological and pharmacokinetic assays of telomerase-specific replication-selective adenovirus. *Cancer Sci* 2008;99:385-90.
- Nemunaitis J, Tong AW, Nemunaitis M, Senzer N, Phadke AP, Bedell C, et al. A phase I study of telomerase-specific replication-competent oncolytic adenovirus (Telomelysin) for various solid tumors. *Mol Ther* 2010;18:429-34.
- Aragona M, Maisano R, Panetta S, Giudice A, Morelli M, La Torre I, et al. Telomere length maintenance in aging and carcinogenesis. *Int J Oncol* 2000;17:981-9.
- Reddel RR. Alternative lengthening of telomeres, telomerase, and cancer. *Cancer Lett* 2003;194:155-63.
- Bryan TM, Englezou A, Dalla-Pozza L, Dunham MA, Reddel RR. Evidence for an alternative mechanism for maintaining telomere length in human tumors and tumor-derived cell lines. *Nat Med* 1997;3:1271-4.
- Henson JD, Neumann AA, Yeager TR, Reddel RR. Alternative lengthening of telomeres in mammalian cells. *Oncogene* 2002;21:598-610.
- Cesare AJ, Reddel RR. Alternative lengthening of telomeres: models, mechanisms and implications. *Nat Rev Genet* 2010;11:319-30.
- Henson JD, Hannay JA, McCarthy SW, Royds JA, Yeager TR, Robinson RA, et al. A robust assay for alternative lengthening of telomeres in sarcomas and astrocytomas. *Clin Cancer Res* 2005;11:217-25.
- Matsuo T, Shimose S, Kubo T, Fujimori J, Yasunaga Y, Ochi M. Telomeres and telomerase in sarcomas. *Anticancer Res* 2009;29:3833-6.
- Bergelson JM, Cunningham JA, Droguett G, Kurt-Jones EA, Krithivas A, Hong JS, et al. Isolation of a common receptor for coxsackie B viruses and adenoviruses 2 and 5. *Science* 1997;275:1320-3.
- Fuxe J, Liu L, Malin S, Philipson L, Collins VP, Pettersson RF. Expression of the coxsackie and adenovirus receptor in human astrocytic tumors and xenografts. *Int J Cancer* 2003;103:723-9.
- Marsee DK, Vadysirisack DD, Morrison CD, Prasad ML, Eng C, Duh QY, et al. Variable expression of coxsackie-adenovirus receptor in thyroid tumors: implications for adenoviral gene therapy. *Thyroid* 2005;15:977-87.
- Anders M, Rösch T, Küster K, Becker I, Höfler H, Stein HJ, et al. Expression and function of the coxsackie and adenovirus receptor in Barrett's esophagus and associated neoplasia. *Cancer Gene Ther* 2009;16:508-15.
- Korn WM, Macal M, Christian C, Lacher MD, McMillan A, Rauen KA, et al. Expression of the coxsackievirus- and adenovirus receptor in gastrointestinal cancer correlates with tumor differentiation. *Cancer Gene Ther* 2006;13:792-7.
- You Z, Fischer DC, Tong X, Hasenburger A, Aguilar-Cordova E, Kieback DG. Coxsackievirus-adenovirus receptor expression in ovarian cancer cell lines is associated with increased adenovirus transduction efficiency and transgene expression. *Cancer Gene Ther* 2001;8:168-75.
- Rice AM, Currier MA, Adams LC, Bharatan NS, Collins MH, Snyder JD, et al. Ewing sarcoma family of tumors express adenovirus receptors

## Disclosure of Potential Conflict of Interest

Y. Urata is an employee of Oncolys BioPharma, Inc., the manufacturer of OBP-301(Telomelysin). The other authors disclosed no potential conflicts of interest.

## Acknowledgments

The authors thank Dr. Satoru Kyo (Kanazawa University) for providing the OST, HOS, and SaOS-2 cells, Dr. Hiroyuki Kawashima (Niigata University) for providing the NOS-2, NOS-10, NDCS-1, NMS-2, and NMFH-1 cells, and Tomoko Sueishi for her excellent technical support.

## Grant Support

This study was supported by grants-in-aid from the Ministry of Education, Science, and Culture, Japan (T. Fujiwara) and grants from the Ministry of Health and Welfare, Japan (T. Fujiwara).

The costs of publication of this article were defrayed in part by the payment of page charges. This article must therefore be hereby marked *advertisement* in accordance with 18 U.S.C. Section 1734 solely to indicate this fact.

Received August 1, 2010; revised November 4, 2010; accepted November 15, 2010; published OnlineFirst February 16, 2011.



- and are susceptible to adenovirus-mediated oncolysis. *J Pediatr Hematol Oncol* 2002;24:527-33.
29. Kawashima H, Ogose A, Yoshizawa T, Kuwano R, Hotta Y, Hotta T, et al. Expression of the coxsackievirus and adenovirus receptor in musculoskeletal tumors and mesenchymal tissues: efficacy of adenoviral gene therapy for osteosarcoma. *Cancer Sci* 2003;94:70-5.
  30. Gu W, Ogose A, Kawashima H, Ito M, Ito T, Matsuba A, et al. High-level expression of the coxsackievirus and adenovirus messenger RNA in osteosarcoma, Ewing's sarcoma, and benign neurogenic tumors among musculoskeletal tumors. *Clin Cancer Res* 2004;10:3831-8.
  31. Taki M, Kagawa S, Nishizaki M, Mizuguchi H, Hayakawa T, Kyo S, et al. Enhanced oncolysis by a tropism-modified telomerase-specific replication-selective adenoviral agent OBP-405 ("Telomelysin-RGD"). *Oncogene* 2005;24:3130-40.
  32. Kawai A, Ozaki T, Ikeda S, Oda T, Miyazaki M, Sato J, et al. Two distinct cell lines derived from a human osteosarcoma. *J Cancer Res Clin Oncol* 1989;115:531-6.
  33. Kunisada T, Miyazaki M, Mihara K, Gao C, Kawai A, Inoue H, et al. A new human chondrosarcoma cell line (OUMS-27) that maintains chondrocytic differentiation. *Int J Cancer* 1998;77:854-9.
  34. Kawai A, Naito N, Yoshida A, Morimoto Y, Ouchida M, Shimizu K, et al. Establishment and characterization of a biphasic synovial sarcoma cell line, SYO-1. *Cancer Lett* 2004;204:105-13.
  35. Hotta T, Motoyama T, Watanabe H. Three human osteosarcoma cell lines exhibiting different phenotypic expressions. *Acta Pathol Jpn* 1992;42:595-603.
  36. Kudo N, Ogose A, Hotta T, Kawashima H, Gu W, Umezumi H, et al. Establishment of novel human dedifferentiated chondrosarcoma cell line with osteoblastic differentiation. *Virchows Arch* 2007;451:691-9.
  37. Imaizumi S, Motoyama T, Ogose A, Hotta T, Takahashi HE. Characterization and chemosensitivity of two human malignant peripheral nerve sheath tumour cell lines derived from a patient with neurofibromatosis type 1. *Virchows Arch* 1998;433:435-41.
  38. Kawashima H, Ogose A, Gu W, Nishio J, Kudo N, Kondo N, et al. Establishment and characterization of a novel myxofibrosarcoma cell line. *Cancer Genet Cytogenet* 2005;161:28-35.
  39. Livak KJ, Schmittgen TD. Analysis of relative gene expression data using real-time quantitative PCR and the  $2^{-\Delta\Delta C(T)}$  method. *Methods* 2001;25:402-8.
  40. Luu HH, Kang Q, Park JK, Si W, Luo Q, Jiang W, et al. An orthotopic model of human osteosarcoma growth and spontaneous pulmonary metastasis. *Clin Exp Metastasis* 2005;22:319-29.
  41. Kirch HC, Ruschen S, Brockmann D, Esche H, Horikawa I, Barrett JC, et al. Tumor-specific activation of hTERT-derived promoters by tumor suppressive E1A-mutants involves recruitment of p300/CBP/HAT and suppression of HDAC-1 and defines a combined tumor targeting and suppression system. *Oncogene* 2002;21:7991-8000.
  42. Glasspool RM, Burns S, Hoare SF, Svensson C, Keith NW. The hTERT and hTERC telomerase gene promoters are activated by the second exon of the adenoviral protein, E1A, identifying the transcriptional corepressor CtBP as a potential repressor of both genes. *Neoplasia* 2005;7:614-22.
  43. Liu D, Kojima T, Ouchi M, Kuroda S, Watanabe Y, Hashimoto Y, et al. Preclinical evaluation of synergistic effect of telomerase-specific oncolytic virotherapy and gemcitabine for human lung cancer. *Mol Cancer Ther* 2009;8:980-7.
  44. Yokoyama T, Iwado E, Kondo Y, Aoki H, Hayashi Y, Georgescu MM, et al. Autophagy-inducing agents augment the antitumor effect of telomerase-selective oncolytic adenovirus OBP-405 on glioblastoma cells. *Gene Ther* 2008;15:1233-9.
  45. Matsumoto K, Shariat SF, Ayala GE, Rauen KA, Lerner SP. Loss of coxsackie and adenovirus receptor expression is associated with features of aggressive bladder cancer. *Urology* 2005;66:441-6.
  46. Anders M, Vieth M, Röcken C, Ebert M, Pross M, Gretschel S, et al. Loss of the coxsackie and adenovirus receptor contributes to gastric cancer progression. *Br J Cancer* 2009;100:352-9.
  47. Küster K, Koschel A, Rohrer N, Fischer A, Wiedenmann B, Anders M. Downregulation of the coxsackie and adenovirus receptor in cancer cells by hypoxia depends on HIF-1 $\alpha$ . *Cancer Gene Ther* 2010;17:141-6.
  48. Kitazono M, Goldsmith ME, Aikou T, Bates S, Fojo T. Enhanced adenovirus transgene expression in malignant cells treated with the histone deacetylase inhibitor FR901228. *Cancer Res* 2001;61:6328-30.
  49. Goldsmith ME, Kitazono M, Fok P, Aikou T, Bates S, Fojo T. The histone deacetylase inhibitor FK228 preferentially enhances adenovirus transgene expression in malignant cells. *Clin Cancer Res* 2003;9:5394-401.
  50. Watanabe T, Hioki M, Fujiwara T, Nishizaki M, Kagawa S, Taki M, et al. Histone deacetylase inhibitor FR901228 enhances the antitumor effect of telomerase-specific replication-selective adenoviral agent OBP-301 in human lung cancer cells. *Exp Cell Res* 2006;312:256-65.

# Expert Opinion

1. Introduction
2. Role of miRNAs in the gastrointestinal tract
3. Deregulation of miRNAs in gastrointestinal tumors
4. miRNAs as novel biomarkers in gastrointestinal tumors
5. Potential role of miRNAs in cancer gene therapy for gastrointestinal tumors
6. Conclusions
7. Expert opinion

## MicroRNAs as potential target gene in cancer gene therapy of gastrointestinal tumors

Hiroshi Tazawa, Shunsuke Kagawa & Toshiyoshi Fujiwara<sup>†</sup>

<sup>†</sup>Okayama University Graduate School of Medicine, Dentistry and Pharmaceutical Sciences, Department of Gastroenterological Surgery, Okayama, Japan

**Introduction:** MicroRNA (miRNA) is a small non-coding RNA, which negatively regulates the expression of many target genes, thereby contributing to the modulation of diverse cell fates. Recent advances in molecular biology have revealed the potential role of miRNAs in tumor initiation, progression and metastasis. Aberrant regulation of miRNAs has been frequently reported in a variety of cancers, including gastrointestinal tumors, suggesting that cancer-related miRNAs are promising as novel biomarkers for tumor diagnosis and are potential target genes for cancer gene therapy against gastrointestinal tumors.

**Areas covered:** The review focuses on the role of specific miRNAs (*miR-192/194/215* and *miR-7*) in the differentiation of gastrointestinal epithelium and on the role of tumor-suppressive (*miR-34*, *miR-143*, *miR-145*) and oncogenic miRNAs (*miR-21*, *miR-17-92* cluster) in gastrointestinal tumors. Furthermore, the potential role of miRNAs as novel biomarkers and target genes for cancer gene therapy against gastrointestinal tumors are discussed. We will also outline the potential clinical application of miRNAs for tumor diagnosis and cancer gene therapy against gastrointestinal tumors.

**Expert opinion:** Exploration of tumor-related miRNAs would provide important opportunities for the development of novel cancer gene therapies aimed at normalizing the critical miRNAs that are deregulated in gastrointestinal tumors.

**Keywords:** cancer, gastrointestinal tumor, gene therapy, microRNA

*Expert Opin. Biol. Ther.* (2011) **11**(2):145-155

### 1. Introduction

MicroRNA (miRNA) are small non-coding RNAs consisting of 22 nucleotides, which post-transcriptionally suppresses the expression of many target genes by pairing with complementary nucleotide sequences in the 3'-untranslated regions of the target mRNA [1]. Aberrant regulation of miRNAs has been frequently reported in a variety of cancers, including gastrointestinal tumors [2-7]. Recent advances in molecular biology have revealed the potential role of miRNAs in tumor initiation, progression and metastasis [8]. In particular, a number of reports have indicated that miRNA can regulate diverse cell fates including cell proliferation [9], the epithelial-mesenchymal transition [10], apoptosis [11] and senescence [12] in human cancer cells. Analysis of global miRNA expression profiles has revealed that gastrointestinal tumors are strictly distinguished from non-gastrointestinal tumors [2]. Since gastrointestinal epithelium is commonly differentiated from the endoderm during development of the digestive tract [13], many miRNAs may be commonly regulated in the gastrointestinal tract and deregulated in gastrointestinal tumors. In this review, we focus on the functional role of miRNAs in gastrointestinal epithelium and tumors,

**informa**  
healthcare



**Article highlights.**

- Gastrointestinal tumors are strictly distinguished from non-gastrointestinal tumors by analysis of global miRNA expression profiles.
- *miR-192/194/215* and *miR-7* have functional roles in the differentiation of intestinal epithelial cells.
- Tumor-suppressive miRNAs (*miR-34* and *miR-143/145*) and oncogenic miRNAs (*miR-21* and *miR-17-92* cluster) are commonly deregulated in gastrointestinal tumors.
- Detection of aberrant miRNA expression in the blood and stool may be a promising screening system for early detection of gastrointestinal tumors.
- Upregulation of *miR-34* and/or downregulation of *miR-21* may be a promising miRNA-based cancer gene therapy for the treatment of patients with gastrointestinal tumors.

This box summarizes key points contained in the article.

such as human gastric and colon cancers, and discuss a miRNA-based strategy for tumor diagnosis and cancer gene therapy against gastrointestinal tumors.

## 2. Role of miRNAs in the gastrointestinal tract

Recent evidence has shown that miRNAs play critical roles in the differentiation of normal cells into various organs [14]. Recently, *miR-192/194/215* and *miR-7* have been shown to have functional roles in the differentiation of intestinal epithelial cells (Figure 1).

### 2.1 miR-192/194/215

Two miRNA clusters, *miR-192/194-2* and *miR-194-1/215*, are located on the human chromosomes 11q13 and 1q41, respectively. The expression of *miR-194/215* was upregulated during the differentiation of human intestinal epithelial cells [15]. It has been recently shown that *miR-192* is the most highly expressed miRNA in intestinal epithelial cells of mice. In addition, Dicer-deficient mice, which lack the machinery to generate miRNAs, exhibited an impaired intestinal barrier function [16], suggesting crucial roles for miRNAs in the differentiation and function of the intestinal epithelium. Furthermore, miRNA expression profiles also support the idea that *miR-192/194/215* are gastrointestinal-tract-related miRNAs that are more highly expressed in gastrointestinal tumors compared with non-gastrointestinal tumors [2].

The expression of *miR-192/194/215* is modulated by tumor suppressor *p53* [17-19]. Hepatocyte nuclear factor-1 $\alpha$  can also play a role in the regulation of *miR-194* expression [15]. The miRNAs *miR-192/194/215* induce cell cycle arrest and cell detachment through suppression of many target genes including cell division cycle 7 (*CDC7*), excision repair cross-complementing 3 (*ERCC3*) and

dihydrofolate reductase (*DHFR*) [17-19]. A previous report has suggested that *p53* and *p53*-downstream target *p21* genes are upregulated during the differentiation of human intestinal epithelial cells [20]. These reports suggest that *p53*-mediated modulation of *miR-192/194/215* expression is involved in the differentiation of human intestinal epithelial cells.

### 2.2 miR-7

*miR-7* has been shown to be involved in the differentiation of intestinal epithelial cells [21]. *miR-7* induces cell detachment through suppression of the expression of the transmembrane glycoprotein CD98, which regulates intestinal epithelial adhesion through interaction with integrin  $\beta$ 1 [22]. In contrast, the expression levels of *miR-7* in inflamed colon tissues were significantly decreased in the colon tissues of patients with Crohn's disease, which is strongly associated with colon carcinogenesis, compared with those in normal colon tissues [21]. The inflammatory cytokine, IL-1 $\beta$ , can suppress *miR-7* expression but conversely induces CD98 expression [21]. These findings suggest that *miR-7* is involved in the differentiation of intestinal epithelial cells and that *miR-7* downregulation by inflammatory cytokines contributes to colon carcinogenesis.

## 3. Deregulation of miRNAs in gastrointestinal tumors

Deregulation of miRNA in human cancers is associated with transcriptional deregulation, epigenetic alterations, mutations, DNA copy number abnormalities and defects in the miRNA biogenesis machinery [23]. Tumor-suppressive miRNAs (*miR-34* and *miR-143/145*) and oncogenic miRNAs (*miR-21* and *miR-17-92* cluster) are commonly deregulated in gastrointestinal tumors (Table 1).

### 3.1 Tumor-suppressive miRNAs

#### 3.1.1 miR-34

The *miR-34* family (*miR-34a*, *-34b* and *-34c*) is a family of tumor suppressive miRNAs that are induced by the tumor suppressor *p53* gene [12,24-27]. We previously reported that *miR-34a* expression was downregulated in 9 (36%) out of 25 human colon cancer tissues compared with the corresponding normal tissues [12]. There are three possible molecular mechanisms of *miR-34* downregulation in human cancer cells as follows; i) *p53* dysfunction, ii) promoter methylation, iii) chromosomal deletion (Figure 2). In more than 50% of human gastrointestinal tumors, the function of the tumor suppressor *p53* is frequently lost due to mutations [28-30] or deletions of chromosome 17p13 [31-33], on which the *p53* gene is located. Recently, frequent promoter hypermethylation of *miR-34a* was observed in a variety of human cancer cells including gastric cancers [34]. The expression of *miR-34b* and *miR-34c* is also downregulated through promoter hypermethylation in human colon cancer



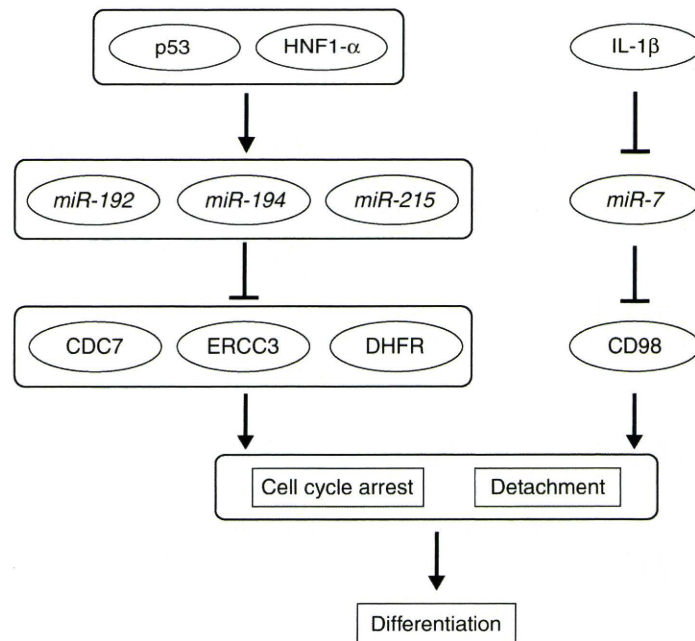


**Figure 1. Functional roles of *miR-192/194/215* and *miR-7* in the differentiation of human intestinal epithelial cells.** Induction of *miR-192/194/215* expression by p53 or HNF-1 $\alpha$  downregulates common target genes (*CDC7*, *ERCC3* and *DHFR*) and induces cell cycle arrest and cell detachment, leading to cell differentiation. Cell detachment and differentiation are also induced through suppression of *CD98* by *miR-7*, which can be inhibited by the inflammatory cytokine IL-1 $\beta$ .

tissues and cell lines, although normal colon tissues show no methylation [35]. Furthermore, the location of miRNA on human chromosomes has been reported to be associated with the fragile chromosomal sites that have been detected in a variety of human cancers [36]. *miR-34a* is located on human chromosome 1p36, which is frequently deleted in gastrointestinal tumors [37]. In contrast, *miR-34b/34c* is located on human chromosome 11q23, which is a fragile site that is associated with breast and lung cancers [36] and that has recently been identified as a colorectal cancer susceptibility locus in a genome-wide association study [38]. These reports suggest that the expression of the *miR-34* family is frequently downregulated through transcriptional deregulation and chromosomal instability in gastrointestinal tumors.

Overexpression of *miR-34a* induces cell cycle arrest, senescence and apoptosis in human cancer cells (Figure 3) [12,24-27]. Regarding the molecular mechanism that underlies *miR-34a*-mediated induction of senescence-like growth arrest, we previously showed that *miR-34a* causes the downregulation of E2F-related genes and the upregulation of p53-related genes in human colon cancer cells [12]. *miR-34a* directly suppresses the expression of E2F3 [39], leading to downregulation of E2F1 and E2F2 [12]. In contrast, direct suppression of sirtuin 1 (SIRT1) expression by *miR-34a* induces p53 activation that functions as a positive-feedback loop [40] and

subsequently upregulates p53-downstream target genes including *p21* [12,40]. Furthermore, the genes encoding the antiapoptotic factor B-cell leukaemia/lymphoma protein2 (BCL2) and the cell cycle-dependent kinase CDK6 are also targeted by *miR-34a* resulting in the induction of apoptosis and cell cycle arrest, respectively [26,41]. Overexpression of *miR-34b* and *miR-34c* in human cancer cells also induces cell cycle arrest, senescence and apoptosis through downregulation of the same target genes as *miR-34a* [42]. These results suggest that *miR-34* plays tumor suppressive roles including the induction of senescence, apoptosis and cell cycle arrest, in human cancer cells. Thus, *miR-34* alteration may induce aberrant cell proliferation, thereby contributing to tumor development in gastrointestinal tracts.

### 3.1.2 *miR-143/145*

The *miR-143/145* cluster is located on human chromosome 5q33 [43]. Gastrointestinal tumors show reduced expression of *miR-143/145* [44-47]. Although the molecular mechanism of *miR-143/145* downregulation remains unclear, recent reports have shown that the tumor suppressor p53 induces expression of *miR-143/145* [48,49], suggesting that *miR-143/145*, similar to *miR-34*, is downregulated following loss of p53 function. *miR-143* suppresses the expression of *KRAS* [50] and DNA methyltransferase 3A [51], whereas *miR-145* downregulates the expressions of oncogenic